

contained *HBII-52*, *HBII-438B*, *UBE3A*, *ATP10C*, and a part of *GABRB3* (Fig. 1B). Proximal and distal breakpoints were not related to any of PWS/AS-related LCRs [Christian et al., 1999]. It was surprising that the sequences were completely identical to those found in the family previously described [Greger et al., 1993]. Relationship of the two families could not be confirmed. However, coincidence of proximal and distal deletion breakpoints as well as inserted 15 nucleotides strongly suggests that the two families originated from the same ancestor. Both families indeed live in neighboring prefectures in Japan.

Phenotype of the proband is compatible to AS and was similar to that of the patient with the identical deletion described by Saitoh et al. [1992] (detailed clinical information was described by Sugimoto et al. [1992]) (Table I). As his mother inherited the deletion from his maternal grandfather, she may suffer from some of PWS features if the deletion contains a gene(s) for PWS. She was carefully evaluated with regard to diagnostic criteria for PWS [Holm et al., 1993]. Only one major criterion (genetic microdeletion) and one minor (myopia) were recognized, thus PWS was definitely unlikely. This

is consistent with the previous finding that a clinically healthy mother of three AS sibs, all sharing an identical deletion [Saitoh et al., 1992; Sugimoto et al., 1992].

Recently brain-specific snoRNA *HBII-52* was found to regulate alternative splicing of serotonin receptor 2C, possibly influencing the serotonin response [Kishore and Stamm, 2006]. Clustering 47 copies of *HBII-52* are maternally imprinted and are suggested to play an important role in pathogenesis of PWS [Cavaille et al., 2000]. However in this family as well as the previously described family [Saitoh et al., 1992], two healthy mothers possessed the microdeletion inherited from their fathers and the deletion included the complete *HBII-52* locus. Thus, the normal phenotype of the mother described here again supports that *HBII-52* does not play any roles in PWS. Similarly the paternally inherited 570-kb deletion in a healthy mother also included *HBII-52* [Burger et al., 2002; Runte et al., 2005]. Rare balanced translocations involving paternal 15q11-q13 in PWS and rare atypical microdeletions now delimit the PWSCR to a 121-kb region covering *HBII-438A* and *HBII-85* clusters [Wirth et al., 2001; Gallagher et al., 2002].

TABLE I. Phenotype of the Proband and Cases Previously Reported

Patient	Proband	Patient 1 ^a [Saitoh et al., 1992]	B-5490 [Burger et al., 2002]
Psychomotor development			
Mental retardation	Severe	Yes	Yes
Absence of speech	Yes	Yes	Yes
Able to speak single word	No	No	No
Able to make sound	Yes		
Able to use sign language	Yes (only at urination)		
Age walked alone	2 years 7 months		1 year 6 months
Neurological features			
Epilepsy	Yes	Yes	
EEG	Abnormal	Abnormal	No
Ataxia (When excited/running) (not marked)	Yes	Yes	Yes
Wide-based gait	Yes		
Flapping hands (when excited/running)	Yes (slightly)	Yes	
Behavior			
Happy disposition	Yes		
Characteristic laughter	No	Yes	Yes
Physical features			
Prominent mandible	Yes	Mild	
Small widely spaced teeth	Yes		Yes
Large mouth	Yes		No
Protruding tongue	Yes (slightly)	Yes	Yes
Small head (<25th percentile)	Yes	Yes	Yes
Occiput	Normal	Flat	
Squint	Yes	Yes	
Weight	Within 90 percentile		-0.2 SD
Height	Within 90 percentile		+0.8 SD
Hypopigmentation	No	No	No
Miscellaneous			
Sleep	Disrupted		
Mouthing	No		
Dribbling/drooling	Yes		
Other	Father is dead (Biliary atresia)		

This table is made with reference to a paper by Fung et al. [1998].

^aClinical information of Patient 1 and his affected sibs was described in a paper by Sugimoto et al. [1992].

In conclusion, a very rare identical 1,487-kb deletion was found in two families possibly originating from the same ancestor. It should be stressed that the deletion can be inherited without any symptoms through paternal lines. Finally *HBII-52* may not be important for PWS pathogenesis.

ACKNOWLEDGMENTS

Research grant from the Ministry of Health, Labour and Welfare for N.M., Grant-in-Aid for Scientific Research on Priority Areas (Research on Pathomechanisms of Brain Disorders) for N.M., Research Promotion Fund from Yokohama Foundation for Advancement of Medical Science for N.M., Natural Science Research Fund from the Mitsubishi Foundation for N.M., and SORST from Japan Science and Technology Agency (JST) for N.N.

REFERENCES

- Boehm D, Herold S, Kuechler A, Liehr T, Laccone F. 2004. Rapid detection of subtelomeric deletion/duplication by novel real-time quantitative PCR using SYBR-green dye. *Hum Mutat* 23:368-378.
- Burger J, Horn D, Tonnie H, Neitzel H, Reis A. 2002. Familial interstitial 570 kbp deletion of the UBE3A gene region causing Angelman syndrome but not Prader-Willi syndrome. *Am J Med Genet* 111:233-237.
- Buxton JL, Chan CT, Gilbert H, Clayton-Smith J, Burn J, Pembrey M, Malcolm S. 1994. Angelman syndrome associated with a maternal 15q11-13 deletion of less than 200 kb. *Hum Mol Genet* 3:1409-1413.
- Cavaille J, Buiting K, Kieffmann M, Lalonde M, Brannan CI, Horsthemke B, Bachelier JP, Brosius J, Huttenhofer A. 2000. Identification of brain-specific and imprinted small nucleolar RNA genes exhibiting an unusual genomic organization. *Proc Natl Acad Sci USA* 97:14311-14316.
- Christian SL, Fantes JA, Mewborn SK, Huang B, Ledbetter DH. 1999. Large genomic duplications map to sites of instability in the Prader-Willi/Angelman syndrome chromosome region (15q11-q13). *Hum Mol Genet* 8:1025-1037.
- Clayton-Smith J, Laan L. 2003. Angelman syndrome: A review of the clinical and genetic aspects. *J Med Genet* 40:87-95.
- Fung DC, Yu B, Cheong KF, Smith A, Trent RJ. 1998. UBE3A "mutations" in two unrelated and phenotypically different Angelman syndrome patients. *Hum Genet* 102:487-492.
- Gallagher RC, Pils B, Albalwi M, Francke U. 2002. Evidence for the role of PWCRI/HBII-85 C/D box small nucleolar RNAs in Prader-Willi syndrome. *Am J Hum Genet* 71:669-678.
- Greger V, Woolf E, Lalonde M. 1993. Cloning of the breakpoints of a submicroscopic deletion in an Angelman syndrome patient. *Hum Mol Genet* 2:921-924.
- Holm VA, Cassidy SB, Butler MG, Hanchett JM, Greenswag LR, Whitman BY, Greenberg F. 1993. Prader-Willi syndrome: Consensus diagnostic criteria. *Pediatrics* 91:398-402.
- Kishore S, Stamm S. 2006. The snoRNA HBII-52 regulates alternative splicing of the serotonin receptor 2C. *Science* 311:230-232.
- Kubota T, Das S, Christian SL, Baylin SB, Herman JG, Ledbetter DH. 1997. Methylation-specific PCR simplifies imprinting analysis. *Nat Genet* 16:16-17.
- Miyake N, Shimokawa O, Harada N, Sosenkina N, Okubo A, Kawara H, Okamoto N, Kurosawa K, Kawame H, Iwakoshi M, Kosho T, Fukushima Y, Makita Y, Yokoyama Y, Yamagata T, Kato M, Hiraki Y, Nomura M, Yoshiura K, Kishino T, Ohta T, Mizuguchi T, Niikawa N, Matsumoto N. 2006. BAC array CGH reveals genomic aberrations in idiopathic mental retardation. *Am J Med Genet Part A* 140A:205-211.
- Runte M, Varon R, Horn D, Horsthemke B, Buiting K. 2005. Exclusion of the C/D box snoRNA gene cluster HBII-52 from a major role in Prader-Willi syndrome. *Hum Genet* 116:228-230.
- Saitoh S, Kubota T, Ohta T, Jinno Y, Niikawa N, Sugimoto T, Wagstaff J, Lalonde M. 1992. Familial Angelman syndrome caused by imprinted submicroscopic deletion encompassing GABAA receptor beta 3-subunit gene. *Lancet* 339:366-367.
- Sugimoto T, Yasuhara A, Ohta T, Nishida N, Saitoh S, Hamabe J, Niikawa N. 1992. Angelman syndrome in three siblings: Characteristic epileptic seizures and EEG abnormalities. *Epilepsia* 33:1078-1082.
- Sutcliffe JS, Jiang YH, Galijaard RJ, Matsuura T, Fang P, Kubota T, Christian SL, Bressler J, Cattanch B, Ledbetter DH, Beaudet AL. 1997. The E6-Ap ubiquitin-protein ligase (UBE3A) gene is localized within a narrow Angelman syndrome critical region. *Genome Res* 7:368-377.
- Wirth J, Back E, Huttenhofer A, Nothwang HG, Lich C, Gross S, Menzel C, Schinzel A, Kioschis P, Tommerup N, Ropers HH, Horsthemke B, Buiting K. 2001. A translocation breakpoint cluster disrupts the newly defined 3' end of the SNURF-SNRPN transcription unit on chromosome 15. *Hum Mol Genet* 10:201-210.

Recent progress in genetics of Marfan syndrome and Marfan-associated disorders

Takeshi Mizuguchi · Naomichi Matsumoto

Received: 31 August 2006 / Accepted: 26 September 2006 / Published online: 24 October 2006
© The Japan Society of Human Genetics and Springer-Verlag 2006

Abstract Marfan syndrome (MFS, OMIM #154700) is a hereditary connective tissue disorder, clinically presenting with cardinal features of skeletal, ocular, and cardiovascular systems. In classical MFS, changes in connective tissue integrity can be explained by defects in fibrillin-1, a major component of extracellular microfibrils. However, some of the clinical manifestations of MFS cannot be explained by mechanical properties alone. Recent studies manipulating mouse *Fbn1* have provided new insights into the molecular pathogenesis of MFS. Dysregulation of transforming growth factor beta ($TGF\beta$) signaling in lung, mitral valve and aortic tissues has been implicated in mouse models of MFS. *TGFBR2* and *TGFBR1* mutations were identified in a subset of patients with MFS (MFS2, OMIM #154705) and other MFS-related disorders, including Loeys–Dietz syndrome (LDS, #OMIM 609192) and familial thoracic aortic aneurysms and dissections (TAAD2, #OMIM 608987). These data indicate that genetic heterogeneity exists in MFS and its related conditions and that regulation of $TGF\beta$ signaling plays a significant role in these disorders.

Keywords Marfan syndrome · *FBN1* · *TGFBR1* · *TGFBR2* · $TGF\beta$ signaling · Genetic heterogeneity · Loeys–Dietz syndrome · Familial thoracic aortic aneurysms and dissections

Introduction

Marfan syndrome (MFS, OMIM #154700) is a connective tissue disorder with autosomal dominant inheritance. MFS is clinically diagnosed according to the Ghent criteria, which describe pleiotropic manifestations affecting multiple organs (De Paepe et al. 1996). Typical MFS can affect the skeletal system (marfanoid habitus including arachnodactyly, dolichostenomelia, pectus deformity and scoliosis), the ocular system (ectopia lentis) and the cardiovascular system (aortic aneurysm/dissection and mitral regurgitation), as well as other systems, including lung, skin, integument, and dura mater. Significant phenotypic variability of MFS is commonly observed between affected members of different families and even among affected members within a single family. Neonatal MFS (nMFS) is the most severe type of MFS and is characterized by severe atrioventricular valve dysfunction, arachnodactyly, joint contracture, crumpled ears and pectus deformity. In addition to classic MFS, incomplete forms of MFS are seen, in which symptoms overlap with those of MFS but the phenotypes do not satisfy the Ghent criteria.

This review focuses on the recent advances in the genetics of MFS and its associated conditions, including Loeys–Dietz syndrome, non-syndromic thoracic aortic aneurysms and dissections, and Shprintzen–Goldberg craniosynostosis syndrome. Abnormal

T. Mizuguchi · N. Matsumoto (✉)
Department of Human Genetics,
Yokohama City University Graduate School of Medicine,
Fukuura 3-9, Kanazawa-ku, Yokohama 236-0004, Japan
e-mail: naomat@yokohama-cu.ac.jp

T. Mizuguchi · N. Matsumoto
Solution-Oriented Research for Science
and Technology (SORST), JST, Kawaguchi, Japan

transforming growth factor beta (TGF β) signaling will be discussed as the core pathogenesis of MFS.

Genetics of Marfan syndrome and its related disorders

FBNI mutation-related disorders

Marfan syndrome

Molecular diagnosis of MFS became possible after mutations had been identified in the *FBNI* gene (Dietz et al. 1991; Lee et al. 1991). *FBNI* is a 230 kb gene, containing 65 exons, which encodes the structural protein fibrillin-1 (Corson et al. 1993). More than 600 *FBNI* mutations are registered in the UMD-*FBNI* database for MFS and its associated disorders (<http://www.umd.be:2030/>) (Collod-Beroud et al. 2003). The mutation detection rate of *FBNI* in MFS varies among studies, ranging from 9% to 91% (Katzke et al. 2002; Loeys et al. 2004; Tynan et al. 1993). This variability could be explained, in part, by the different techniques used, but the most significant influencing factor is likely to be sample bias. The frequencies are quite different between patients fulfilling the Ghent criteria and those not fulfilling them (Biggin et al. 2004; Halliday et al. 2002; Loeys et al. 2001; Rommel et al. 2002, 2005; Tynan et al. 1993).

Extensive mutational analyses failed to show *FBNI* involvement in almost 10% or more of patients with MFS satisfying the Ghent criteria. Although one possible explanation could be due to so-called missing mutations in the promoter region or in other non-coding sequences, the existence of a second locus for MFS (*MFS2*) was hypothesized (Collod et al. 1994; Dietz et al. 1995; Gilchrist 1994). In 2004, patients with *MFS2* were shown to have mutations in the *TGFBR2* gene, which encodes the transmembrane receptor type II of TGF β (Mizuguchi et al. 2004). *TGFBR2* mutations were later linked to other clinically overlapping syndromes, described below (Kosaki et al. 2006; Loeys et al. 2005; Pannu et al. 2005a).

Other fibrillinopathies

FBNI mutations were also found in incomplete forms of MFS as well as in several other MFS-related disorders such as nMFS, isolated ectopia lentis, Shprintzen–Goldberg craniosynostosis syndrome (SGS), familial thoracic aortic aneurysms and dissections (TAAD), and autosomal dominant Weill–Marchesani syndrome (Table 1) (Faivre et al. 2003; Francke et al. 1995; Kainulainen et al. 1994; Milewicz et al. 1996; Sood

et al. 1996). This resulted in the recognition of “fibrillinopathies” caused by *FBNI* aberrations (Charbonneau et al. 2004).

TGFBR mutation-related disorders

Marfan syndrome type 2

In 1993 Boileau et al. (1993) reported a large French family (MS1 family) with a Marfan-like phenotype that was not linked to the *FBNI* locus. The syndrome was subsequently designated Marfan syndrome type 2 (*MFS2*, OMIM #154705). In this review we are defining *MFS2* genetically (not clinically) as the classic MFS phenotype (based on the Ghent criteria) caused by mutation in the *TGFBR2* locus.

Marfan-like symptoms observed in this family consisted of severe cardiovascular findings, including sudden death of affected members at young age, probably due to a thoracic aortic dissection, and typical MFS skeletal features, but no significant ocular findings were seen. However, one affected family member (IV-83 from the large French family, MS1) was recently reported to suffer from ectopia lentis, which is clinically compatible with classic MFS according to the Ghent criteria but surprising in light of the absence of the condition in other family members (Mizuguchi et al. 2004). Clinical re-evaluation of this individual as well as other affected members is warranted.

Genetic analysis of the French family enabled a successful mapping of the second locus for MFS (*MFS2*) to 3p24.2-p25 (Collod et al. 1994). A Japanese boy with MFS was later shown to have de novo complex chromosomal rearrangements involving 3p24.1, which is close to the *MFS2* locus (Mizuguchi et al. 2004). Detailed genomic analysis revealed that the 3p24.1 breakpoint disrupted the *TGFBR2* gene. Subsequent *TGFBR2* sequence analysis in the MS1 family identified in all affected members a nucleotide substitution c.1524G > A (p.Q508Q) of *TGFBR2*, which is

Table 1 Marfan syndrome-related disorders and mutated genes

Disorder	Gene
Marfan syndrome	<i>FBNI</i> , <i>TGFBR1</i> , <i>TGFBR2</i>
Neonatal Marfan syndrome	<i>FBNI</i>
Familial thoracic aortic aneurysms and dissections	<i>FBNI</i> , <i>TGFBR1</i> , <i>TGFBR2</i>
Isolated ectopia lentis	<i>FBNI</i>
Shprintzen–Goldberg craniosynostosis syndrome	<i>FBNI</i> , <i>TGFBR2</i>
Autosomal dominant Weill–Marchesani syndrome	<i>FBNI</i>
Loyes–Dietz syndrome	<i>TGFBR1</i> , <i>TGFBR2</i>

hypothesized to result in protein truncation due to abnormal splicing. Further analysis of 19 unrelated probands unlinked to *FBNI* identified c.923T > C (p.L308P), c.1346C > T (p.S449F) and c.1609C > T (p.R537C; recurrent in two independent families) (Table 2 and Fig. 1). These missense mutations affect an evolutionarily conserved amino acid in the serine/threonine kinase domain of TGF β receptor type II. This finding confirmed that the MFS phenotype can be caused not only by mutations in *FBNI* but also by mutations in *TGFBR2*.

Loeys–Dietz syndrome

Loeys et al. (2005) reported a new aortic aneurysm syndrome presenting with cardiovascular and skeletal manifestations consistent with those seen in MFS, along with other features not present in MFS. Loeys–Dietz syndrome (LDS, OMIM #609192) is characterized by hypertelorism, bifid uvula, cleft palate, generalized arterial tortuosity, and ascending aortic aneurysm and dissection. Hypothesizing that abnormal TGF β signaling might cause vascular and craniofacial phenotypes, Loeys et al. (2005) investigated *TGFBR2* as a candidate gene for LDS. Heterozygous *TGFBR2* mutations were found in six of ten LDS patients: five missense mutations in the serine/threonine kinase domain [c.1006T > A (p.Y336N), c.1063G > C (p.A355P), c.1069G > T (p.G357W), c.1582C > T (p.R528C), c.1583G > A (p.R528H)], as seen in MFS2, and a single mutation in a splice-acceptor site (IVS1-2A > G) (Table 2, Fig. 1). The remaining four patients were shown to have *TGFBR1* mutations: three missense mutations in the serine/threonine kinase domain [c.953T > G (p.M318R), c.1199A > G (p.D400G) and c.1460G > C (p.R487P)] and a missense mutation in the glycine/serine-rich (GS) domain [c.599C > T (p.T200I)] (Table 2, Fig. 1). Owing to the clinical overlap of MFS and Shprintzen–Goldberg craniosynostosis syndrome (SGS) with LDS, Loeys et al. (2005) also screened seven MFS patients (unlinked to *FBNI*) and five SGS patients for mutations in *TGFBR1* and *TGFBR2*, but no abnormalities were seen at these loci.

Two other *TGFBR2* mutations [c.773T > G (p.V258G) and c.1067G > C (p.R356P)] and another *TGFBR1* mutation [c.722C > T (p.S241L)] have since been reported in other patients meeting the clinical description of LDS by other groups (Table 2, Fig. 1) (Ki et al. 2005; Matyas et al. 2006). Finally, Loeys et al. (2006) collected 30 more probands of LDS and found *TGFBR2* mutations in 21 and *TGFBR1* mutations in nine (Table 2, Fig. 1) (Loeys et al. 2006). Furthermore, LDS type II (LDS2) without craniofacial features was

also proposed. Eight *TGFBR2* and four *TGFBR1* mutations were found in LDS2 patients (Tables 2 and 3, Fig. 1) (Loeys et al. 2006).

Familial thoracic aortic aneurysms and dissections

Non-syndromic thoracic aortic aneurysms and dissections (TAAD) have complex and heterogeneous etiology, with some families inheriting TAAD in an autosomal dominant fashion, with decreased penetrance and variable expression. To date, at least three TAAD loci have been mapped by linkage studies of large single families (Pannu et al. 2005b): *TAAD1* at 5q13–q14 (Guo et al. 2001), the familial aortic aneurysm 1 locus (*FAA1*) at 11q23–q24 (Vaughan et al. 2001), and *TAAD2* at 3p24–p25 (Hasham et al. 2003).

The realization that *TAAD2* (OMIM, #608987) and MFS2 are clinically overlapping diseases that both map to 3p24–p25 led Pannu et al. (2005a) to look for *TGFBR2* mutations in 80 unrelated TAAD families, including the large family with disease linkage to 3p24–p25. Two *TGFBR2* mutations [c.1378C > T (p.R460C) and c.1379G > A (p.R460H)], both affecting the same amino acid residue in the serine/threonine kinase domain, were identified in four families, or approximately 5% of the TAAD cases (Pannu et al. 2005a) (Table 2, Fig. 1). Each mutation occurred in the unique haplotype block, indicating an independent mutation event.

The mutational hotspot at the p.R460 residue in *TAAD2* suggested a positive phenotype–genotype correlation, and this observation was supported by the discovery of another family with p.R460H that was initially diagnosed as having *TAAD2* and, later, as having a distinctive condition with cardiovascular findings consistent with *TAAD2*, together with arterial tortuosity and aneurysm (Law et al. 2005, 2006). Three additional missense *TGFBR2* mutations [c.1159G > A (p.V387G), c.1181G > A (p.C394Y), c.1657T > A (p.S553T)] and, more importantly, one *TGFBR1* mutation [c.1460G > A (p.R487Q)] were found in four TAAD patients (Matyas et al. 2006).

Shprintzen–Goldberg craniosynostosis syndrome

Shprintzen–Goldberg craniosynostosis syndrome (SGS, OMIM, #182212) is characterized by craniosynostosis and other craniofacial features, marfanoid skeletal abnormalities, and developmental delay (Robinson et al. 2005). Furlong syndrome (FS) is a similar marfanoid disorder with craniosynostosis, which differs from SGS by the absence of mental retardation (Furlong et al. 1987).

Table 2 Summary of *TGFBR2* and *TGFBR1* mutations

Gene	Disorder	Exon	Mutations	Domain	Splicing abnormality	Nature	Ghent criteria	References	
<i>TGFBR2</i>	MFS	–	Chromosomal rearrangements	–	–	De novo	Fulfilled	Mizuguchi et al. (2004)	
		4	c.923T > C (p.L308P)	Kinase	–	De novo	Fulfilled	Mizuguchi et al. (2004)	
		4	c.1067G > C (p.R356P)	Kinase	–	De novo	Not fulfilled ^a	Sakai et al. (2006)	
		4	c.1106G > T (p.G369V) and c.1159G > C (p.V387L) ^b	Kinase	–	Familial	Not fulfilled	Matyas et al. (2006)	
		4	c.1151A > G (p.N384S)	Kinase	–	Familial	Not fulfilled	Singh et al. (2006)	
		4	c.1188T > G (p.C396W) and c.-334T > A ^c	Kinase	–	De novo	Fulfilled	Singh et al. (2006)	
		5	c.1273A > G (p.M425V)	Kinase	–	Familial	Fulfilled	Disabella et al. (2006)	
		5	c.1336G > A (p.D446N)	Kinase	–	De novo	Not fulfilled	Disabella et al. (2006)	
		5	c.1336G > A (p.D446N)	Kinase	–	De novo	Not fulfilled ^a	Sakai et al. (2006)	
		5	c.1322C > T (p.S441F)	Kinase	–	De novo	Not fulfilled	Singh et al. (2006)	
		5	c.1346C > T (p.S449F)	Kinase	–	Familial	Not fulfilled	Mizuguchi et al. (2004)	
		5	c.1378C > T (p.R460C)	Kinase	–	Familial	Fulfilled	Singh et al. (2006)	
		5	c.1379G > A (p.R460H)	Kinase	–	Familial	Fulfilled	Disabella et al. (2006)	
		6	c.1489C > T (p.R497X)	Kinase	–	De novo?	Not fulfilled	Singh et al. (2006)	
		6	c.1524G > A (p.Q508Q)	Kinase	+	Familial	Fulfilled	Mizuguchi et al. (2004)	
		7	c.1561T > C (p.W521R)	Kinase	–	De novo	Fulfilled	Matyas et al. (2006)	
		7	c.1609C > T (p.R537C)	Kinase	–	Familial	Fulfilled	Mizuguchi et al. (2004)	
		LDS	–	IVS1-2A > G	–	+	De novo?	–	Loeys et al. (2005)
			4	c.773T > G (p.V258G)	Kinase	–	Familial	Fulfilled	Matyas et al. (2006)
	4		p.A329T	Kinase	–	?	–	Loeys et al. (2006)	
	4		c.1006T > A (p.Y336N)	Kinase	–	Familial	–	Loeys et al. (2005)	
	4		c.1063G > C (p.A355P)	Kinase	–	Familial	–	Loeys et al. (2005)	
	4		c.1067G > C (p.R356P)	Kinase	–	De novo	–	Ki et al. (2005)	
	4		c.1069G > T (p.G357W)	Kinase	–	De novo	–	Loeys et al. (2005)	
	4		p.N384S	Kinase	–	?	–	Loeys et al. (2006)	
	5		p.P427L	Kinase	–	?	–	Loeys et al. (2006)	
	5		p.P427S	Kinase	–	?	–	Loeys et al. (2006)	
	5		p.Y448H	Kinase	–	?	–	Loeys et al. (2006)	
	5		p.S449F	Kinase	–	?	–	Loeys et al. (2006)	
	5		p.M457K	Kinase	–	?	–	Loeys et al. (2006)	
	5		p.R460H	Kinase	–	?	–	Loeys et al. (2006)	
	5		p.C461Y	Kinase	–	?	–	Loeys et al. (2006)	
	–		IVS5-1G > A	–	+	?	–	Loeys et al. (2006)	
	6		p.R495X	Kinase	–	?	–	Loeys et al. (2006)	
	7		p.E519K	Kinase	–	?	–	Loeys et al. (2006)	
	7		p.C520Y	Kinase	–	?	–	Loeys et al. (2006)	
	7		p.D524N	Kinase	–	?	–	Loeys et al. (2006)	
	7		p.A527V	Kinase	–	?	–	Loeys et al. (2006)	
	7		c.1582C > T (p.R528C)	Kinase	–	De novo	–	Loeys et al. (2005, 2006)	
	7		c.1583G > A (p.R528H)	Kinase	–	De novo	–	Loeys et al. (2005, 2006)	
	7		p.L529F	Kinase	–	?	–	Loeys et al. (2006)	
	7		p.C533R	Kinase	–	?	–	Loeys et al. (2006)	
	7		p.C533F	Kinase	–	?	–	Loeys et al. (2006)	
	7		p.R537C	Kinase	–	?	–	Loeys et al. (2006)	
	7		p.R537G	Kinase	–	?	–	Loeys et al. (2006)	
	TAAD	4	c.1159G > A (p.V387M)	Kinase	–	Familial	–	Matyas et al. (2006)	
		4	c.1181G > A (p.C394Y)	Kinase	–	?	–	Matyas et al. (2006)	
5		c.1378C > T (p.R460C)	Kinase	–	Familial	–	Pannu et al. (2005a)		
5		c.1379G > A (p.R460H)	Kinase	–	Familial	–	Pannu et al. (2005a) and Law et al. (2006)		

Table 2 continued

Gene	Disorder	Exon	Mutations	Domain	Splicing abnormality	Nature	Ghent criteria	References
<i>TGFBR1</i>	SGS (LDS?)	7	c.1657T > A (p.S553T)	–	–	De novo?	–	Matyas et al. (2006)
		–	IVS5-2A > G	–	+	De novo	–	Kosaki et al. (2006)
	MFS	4	c.759G > A (p.M253I)	Kinase	–	Familial	Fulfilled	Singh et al. (2006)
		4	c.799A > C (p.N267H)	Kinase	–	Familial	Not fulfilled	Matyas et al. (2006)
	LDS	5	c.934G > A (p.G312S)	Kinase	–	Familial	Fulfilled	Singh et al. (2006)
		7	c.1135A > G (p.M379V)	Kinase	–	?	Not fulfilled	Sakai et al. (2006)
		4	c.599C > T (p.T200I)	GS	–	De novo	–	Loeys et al. (2005)
		4	p.K232E	Kinase	–	?	–	Loeys et al. (2006)
		4	p.F234L	Kinase	–	?	–	Loeys et al. (2006)
		4	c.722C > T (p.S241L)	Kinase	–	De novo	Fulfilled	Loeys et al. (2006) and Matyas et al. (2006)
		5	c.953T > G (p.M318R)	Kinase	–	De novo	–	Loeys et al. (2005)
		6	p.A350E	Kinase	–	?	–	Loeys et al. (2006)
		6	p.G353V	Kinase	–	?	–	Loeys et al. (2006)
6		p.G374E	Kinase	–	?	–	Loeys et al. (2006)	
7	c.1199A > G (p.D400G)	Kinase	–	De novo	–	Loeys et al. (2005)		
9	p.N478S	Kinase	–	?	–	Loeys et al. (2006)		
9	c.1460G > C (p.R487P)	Kinase	–	Familial	–	Loeys et al. (2005, 2006)		
TAAD	9	p.R487Q	Kinase	–	?	–	Loeys et al. (2006)	
	9	p.R487W	Kinase	–	?	–	Loeys et al. (2006)	
	9	c.1460G > A (p.R487Q)	Kinase	–	De novo	–	Matyas et al. (2006)	
	FS	4	c.722C > T (p.S241L)	Kinase	–	De novo	Fulfilled	Ades et al. (2006)

MFS Marfan syndrome, LDS Loeys-Dietz syndrome, TAAD Familial thoracic aortic aneurysms and dissections, SGS Shprintzen-Goldberg craniosynostosis syndrome, FS Furlong syndrome

^a LDS facial features were recognized

^b Two nucleotide changes in one allele

^c Compound heterozygote

Although a question was raised on the involvement of *FBNI* abnormality in SGS (Robinson et al. 2005), at least two *FBNI* mutations were identified (Kosaki et al. 2006; Sood et al. 1996).

Furthermore, the initial study of five SGS patients failed to reveal mutations in either *TGFBR1* or *TGFBR2* (Loeys et al. 2005), but Kosaki et al. (2006) recently reported a *TGFBR2* mutation [IVS5-2A > G] (Table 2, Fig. 1) in an SGS patient with craniofacial and skeletal abnormalities, mild developmental delay, and cardiovascular features, including aortic regurgitation, annuloaortic ectasia and sigmoid configuration of the brachiocephalic, left common carotid and left subclavian arteries. Robinson et al. (2006), however, suggested that this patient might be more appropriately diagnosed as having LDS, due to the presence of bifid uvula and arterial manifestations.

An identical *TGFBR1* mutation [c.722C > T (p.S241L)] was reported in two unrelated patients described as having probable FS (Table 2, Fig. 1) (Ades et al. 2006). One of these patients had learning difficulties, and the other had normal intelligence (Ades et al. 2006). Systemic arterial tortuosity was not evaluated in either of them, but one showed bifid uvula,

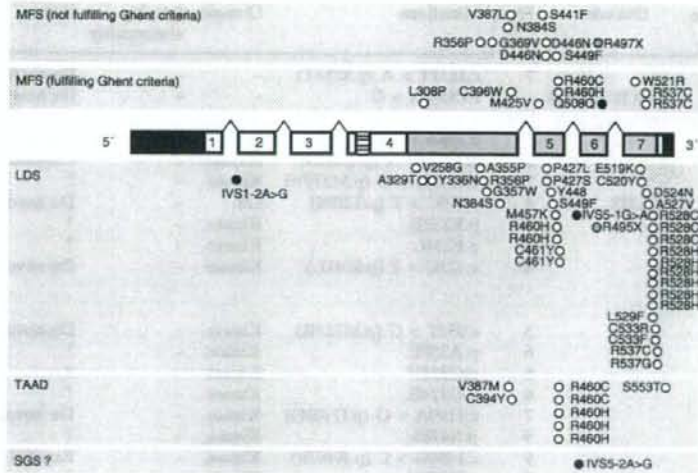
consistent with LDS. The same mutation was also reported in an LDS patient with hypertelorism, tortuous arteries and bifid uvula (Matyas et al. 2006).

Germline *TGFBR* mutations and connective tissue disorders

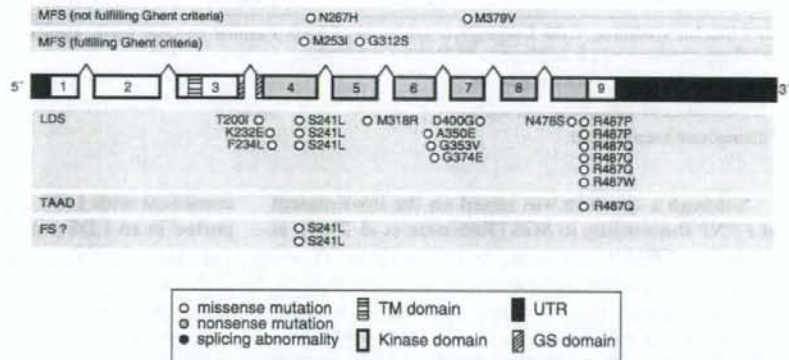
The various mutations, as well as gene disruption by chromosomal structural abnormality, suggest that loss-of-function mutations of *TGFBR2* are responsible for a wide spectrum of connective tissue disorders, but no simple genotype–phenotype correlation has been observed. It is intriguing that domain-specific germline mutations of *TGFBI* cause Camurati–Engelmann disease (CED, OMIM #131300) (Kinoshita et al. 2000) associated with marfanoid habitus, despite the absence of connective tissue fragility. *TGFBI* mutations in CED were shown to cause increased TGF β signaling (Janssens et al. 2003). These findings suggest that abnormal TGF β signaling could be responsible for the skeletal features of MFS. This hypothesis is corroborated by earlier studies describing the roles of TGF β signaling in skeletal development (Alvarez and Serra 2004; Serra et al. 1999).

Fig. 1 Mutation spectrum of *TGFBR2* and *TGFBR1* identified in Marfan syndrome and its related disorders. Numbered boxes indicate exons of each gene. Open and filled circles represent missense and splicing abnormality mutations, respectively. Each mutation was found in a different family. Functional domains are shown as patterned boxes. *MFS* Marfan syndrome, *LDS* Loeys-Dietz syndrome, *TAAD* Familial thoracic aortic aneurysms and dissections, *SGS* Shprintzen-Goldberg craniosynostosis syndrome, *FS* Furlong syndrome

TGFBR2



TGFBR1



TGFBR2 and *TGFBR1* mutations found in MFS and its related disorders are generally associated with severe vascular consequences that differ somewhat from those found in patients with *FBNI* mutations. The vascular consequences associated with *TGFBR2* and *TGFBR1* mutations include aortic dissections in young age and aneurysms at sites distant from the aortic root. Thus, careful screening of arterial tortuosity and aneurysms from head to leg is highly recommended in this patient population.

Whether an MFS2 phenotype exists as a separate disorder from LDS is debatable. *TGFBR1* and *TGFBR2* aberrations are highly prevalent in LDS, which is characterized by severe cardiovascular features and family histories of aortic dissection with sudden death. Following the first report of *TGFBR2*

mutations in MFS (Mizuguchi et al. 2004), LDS, TAAD2, SGS, and FS were recognized as *TGFBR* mutation-related disorders. Although the original MFS2 patients with *TGFBR2* mutations (Mizuguchi et al. 2004) could not be reasonably re-examined for the presence of LDS features such as bifid uvula, hypertelorism, craniosynostosis, and arterial tortuosity, at least three reports have since described *TGFBR1* or *TGFBR2* mutations in classic MFS patients in whom LDS had been ruled out (Disabella et al. 2006; Matyas et al. 2006; Singh et al. 2006). Four missense mutations [c.1273A > G (p.M425V), c.1378C > T (p.R460C), c.1379G > A (p.R460H), and c.1561T > C (p.W521R)] and compound heterozygous mutations [c.1337G > A (p.D446N) and c.-334T > A] in *TGFBR2* were identified in five patients with MFS that satisfied the Ghent

Table 3 Frequency of *TGFBR2/TGFBR1* mutations in MFS-related disorders

Diagnosis	FBNI involvement	Gene tested	Mutations (%)		References
MFS	Negative	TGFBR2	25	(5/20)	Mizuguchi et al. (2004)
	Negative	TGFBR1	0	(0/7)	Loeys et al. (2005)
		TGFBR2	0	(0/7)	
	Negative	TGFBR2	100?	(3/3) ^a	Disabella et al. (2006)
	Negative or unknown	TGFBR2	3	(1/30) ^b	Ki et al. (2005)
	Negative	TGFBR1	5	(2/41)	Singh et al. (2006)
		TGFBR2	12	(5/41)	
LDS	Negative	TGFBR1	5	(1/22)	Sakai et al. (2006)
		TGFBR2	9	(2/22)	
	Unknown	TGFBR1	40	(4/10)	Loeys et al. (2005)
LDS	Unknown	TGFBR2	60	(6/10)	
	Unknown	TGFBR1	30	(9/30)	Loeys et al. (2006)
LDS2	Unknown	TGFBR2	70	(21/30)	
	Unknown	TGFBR1	10	(4/40)	Loeys et al. (2006)
TAAD	Unknown	TGFBR2	20	(8/40)	
	Unknown	TGFBR2	0	(0/10)	Mizuguchi et al. (2004)
SGS	Unknown	TGFBR2	5	(4/80)	Pannu et al. (2005a)
	Unknown	TGFBR1	0	(0/5)	Loeys et al. (2005)
MFS-related phenotypes	Negative	TGFBR2	0	(0/5)	
		TGFBR1	0	(0/1)	Kosaki et al. (2006)
		TGFBR2	100	(1/1)	
MD-CS/MR (FS)	Negative	TGFBR1	100	(2/2) ^c	Ades et al. (2006)
		TGFBR2	0	(0/2)	
MFS-related phenotypes	Negative	TGFBR1	4	(3/70)	Matyas et al. (2006)
		TGFBR2	9	(6/70)	

MFS Marfan syndrome, LDS Loeys-Dietz syndrome, LDS2 Loeys-Dietz syndrome type II, TAAD Familial thoracic aortic aneurysms and dissections, SGS Shprintzen-Goldberg craniosynostosis syndrome, MD-CS/MR Marfan–craniosynostosis/mental retardation, FS Furlong syndrome

^a Total number of patients screened was not described

^b The patient was initially diagnosed as having an MFS variant, which was later refined as LDS

^c The two patients with a *TGFBR1* mutation were categorized to Furlong syndrome

criteria. Seven more patients with MFS that did not satisfy the Ghent criteria were also reported to have mutations in *TGFBR2* (Disabella et al. 2006; Matyas et al. 2006; Sakai et al. 2006; Singh et al. 2006). In addition, two *TGFBR1* missense mutations [c.759G > A (p.M253I) and c.934G > A (p.G312S)] were found in two MFS patients and two *TGFBR1* mutations [c.799A > C (p.N267H) and c.1135A > G (p.M379V)] were identified in two patients not fulfilling MFS. Thus, *TGFBR2* and *TGFBR1* aberrations were observed in typical cases of classic MFS with no signs of LDS (Singh et al. 2006).

However, it should be noted that arterial tortuosity, a cardinal feature of LDS, was not systematically evaluated in any of the four studies (Disabella et al. 2006; Matyas et al. 2006; Sakai et al. 2006; Singh et al. 2006). Moreover, two research groups were unable to identify *TGFBR2* mutations in 29 MFS patients (*FBNI* was normal in 24 and unknown in five) (Ki et al. 2005) and seven patients (*FBNI* was normal) with MFS compatible with the Ghent criteria (Loeys et al. 2005). Thus, the question of whether an MFS2 phenotype and

LDS should be classified as the same disorder remains unresolved.

At least six *TGFBR2* mutations (R356P, N384S, R460H, R460C, S449F, and R537C) and two *TGFBR1* mutations (S241L and R487Q) were recognized in two or three conditions (i.e., R460H found in MFS, LDS, and TAAD) (Ades et al. 2006; Disabella et al. 2006; Ki et al. 2005; Loeys et al. 2006; Matyas et al. 2006; Mizuguchi et al. 2004; Pannu et al. 2005a; Sakai et al. 2006; Singh et al. 2006) (Fig. 1, Table 2), implying that *TGFBR* mutations may cause various clinical consequences or that appropriate diagnosis is rather difficult for these disorders.

Pathogenesis of Marfan syndrome

Fibrillin-1 involvement in connective tissue disorders

Extracellular matrix (ECM) is formed by a number of macromolecules that are secreted and deposited into the space surrounding cells, where they are essential

for tissue development and homeostasis. Fibrillin-1 is an ECM protein that is assembled into microfibrillar networks, where it interacts with other ECM proteins. Fibrillin-rich microfibrils form peripheral components of elastic fibers, which play a role as an architectural foundation and provide elasticity to tissues (Kielty et al. 2002).

Fibrillin-1 is a multi-domain protein that contains three characteristic modules: an epidermal growth factor (EGF)-like motif, a latent TGF β binding protein (LTBP) motif, and a fusion of the two (Fib motif). The majority of the EGF-like modules in the *FBNI* gene have a conserved calcium-binding sequence (cbEGF-like module).

Mutations associated with MFS are distributed over the entire *FBNI* gene. No genotype–phenotype correlation has been clearly established, except for neonatal MFS (nMFS). Most mutations causing nMFS seem to be clustered in exons 24–32, although other phenotypes are also associated with mutations in these exons.

The fibrillin-1 protein contains 47 EGF-like modules, characterized by six cysteine residues that form disulfide bonds with one another. Most MFS missense mutations occur in one of the 43 cbEGF-like modules (Boileau et al. 2005; Robinson and Godfrey 2000). These mutations are thought to influence the protein structure and calcium binding affinity of cbEGF-like modules, with various deleterious effects (Boileau et al. 2005; Downing et al. 1996).

In classical MFS the incidence of ectopia lentis was significantly higher in patients harboring cysteine substitutions in the cbEGF-like modules than in patients with premature termination codon (PTC) mutations (Arbustini et al. 2005; Biggin et al. 2004; Loeys et al. 2004; Rommel et al. 2005; Schrijver et al. 2002). Furthermore, isolated or predominant ectopia lentis is frequently associated with cysteine substitutions (Ades et al. 2004; Comeglio et al. 2002), suggesting that cysteine residues may have a critical function in suspensory ligaments of the eyes, as previously described (Rommel et al. 2005).

The dominant–negative mechanism of mutant fibrillin-1 in MFS pathology is an attractive hypothesis in the light of the polymerizing nature of fibrillin-1 molecules into microfibrils. Various studies have examined the correlation between the expression level of mutant mRNA produced by PTC mutations and the degree of clinical severity (Ades et al. 2004; Dietz et al. 1993; Schrijver et al. 2002). Nonsense-mediated mRNA decay could limit aberrant protein production from mutated alleles in heterozygous patients, but remnant mutant fibrillin-1 proteins may act in a dominant–negative fashion. However, the hypothesized associa-

tion between expression level and clinical severity is controversial. It is also possible that different expression levels of normal *FBNI* alleles leads to different phenotypes in MFS family members sharing the same heterozygous PTC mutation (Hutchinson et al. 2003).

Support for the haploinsufficiency hypothesis as a mechanism in MFS pathogenesis comes from the finding of an *FBNI* deletion in a patient with a number of marfanoid characteristics (Hutchinson et al. 2003; Judge et al. 2004) as well as in mouse models (Judge et al. 2004). In transgenic mice carrying human mutant *FBNI* (p.C1663R), no obvious cardiovascular and skeletal signs have been recognized, despite the co-assembly of the mutant protein into mouse microfibrillar networks. Other knock-in mice (in which the p.C1039G mutation *Fbn1*^{C1039G/+} targeted the endogenous *Fbn1*) showed decreased microfibrillar deposition, skeletal abnormalities and changes in the architecture of the aortic wall. Notably, the aortic wall phenotype was rescued by the wildtype *FBNI* transgene.

TGF β signaling and connective tissue disorders

TGF β is a secreted polypeptide that plays diverse roles in cell proliferation and differentiation, apoptosis, and extracellular matrix formation (Cohen 2003; Derynck et al. 2001; Igotz and Massague 1986; Massague et al. 2000). TGF β 1 is abundant in the ECM. An inactive form of mature TGF β 1 stays in a complex with latency-associated polypeptide (LAP), which is an N-terminal peptide cleaved from proTGF β 1, and latent TGF β binding protein (LTBP). Mature TGF β 1 and LAP are noncovalently associated in a small latency complex (SLC). The SLC binds to LTBP via disulfide bonds between LAP and LTBP, forming a large latency complex (LLC) (Annes et al. 2003). LTBP plays a role in folding and secreting TGF β 1, targeting it appropriately to the ECM, and modulating TGF β activity (Charbonneau et al. 2004; Kaartinen and Warburton 2003; Ramirez et al. 2004; Rifkin 2005).

A recent study revealed that LTBP-1 (one of the LTBPs) and fibrillin interact in vitro and suggested that fibrillin-1 may stabilize the latent TGF β complexes in the ECM (Isogai et al. 2003). Support for this hypothesis is seen in mouse models of MFS. Three strains of transgenic mice, each harboring a different type of *Fbn1* mutation, displayed several MFS features with variable severity (Judge et al. 2004; Pereira et al. 1997, 1999). Increased TGF β activity was observed in at least four organs (lung, mitral valve, aortic and dural tissues), possibly as a result of excess free LLC due to inadequate stabilization within the ECM, as previously hypothesized (Habashi et al. 2006; Jones et al. 2005; Neptune

et al. 2003; Ng et al. 2004; Rifkin 2005). Administration of an anti-TGF β neutralizing antibody rescued the lung, mitral valve, and aortic tissue phenotypes (Habashi et al. 2006; Neptune et al. 2003; Ng et al. 2004). Furthermore, aortic aneurysm was prevented by the administration of losartan, an angiotensin II type 1 receptor blocker that alleviates increased TGF β activity (Habashi et al. 2006). Taken together, these findings support an association of abnormal TGF β signaling with MFS pathogenesis. Interaction between the affected structural ECM components and aberrant TGF β signaling may coordinately determine MFS phenotypes.

TGF β transduces its signals via two distinct types of transmembrane receptors, type I (T β RI) and type II (T β RII), encoded by *TGFBR1* and *TGFBR2*, respectively (ten Dijke et al. 1996; Wrana et al. 1994). Both types of receptors consist of an extracellular domain, a transmembrane domain and a serine/threonine kinase domain. A glycine/serine-rich domain (GS domain) is specific for T β RI. The ligand-bound T β RII phosphorylates the GS domain, which then acts in signal transduction (Wieser et al. 1995).

It is likely that abnormal TGF β signaling is involved in the human MFS phenotype. Identification of *TGFBR2* mutations in MFS2 supports the hypothesis and provided the first direct link between a human connective tissue disorder and abnormal TGF β signaling. Loss-of-function *TGFBR2* mutations are hypothesized to cause MFS2, LDS and TAAD2. In our previous study mammalian cells were transfected with MFS2-related mutant *TGFBR2* constructs, and a luciferase assay clearly showed decreased TGF β signaling activity (Mizuguchi et al. 2004). If the highly conserved p.R460 residue is essential for the structural integrity of the catalytic loop of T β RII, the p.R460 missense mutations found in TAAD2 could dramatically perturb TGF β signaling (Pannu et al. 2005a).

By contrast, aortic tissues from LDS individuals showed increased TGF β signaling activity. The heterozygous state (with one normal allele and the other mutant) of *TGFBR2* abnormality in affected individuals might not simply reflect a loss-of-function nature of the mutation, probably because of the complex regulation of the TGF β signaling pathway (Loeys et al. 2005). Paradoxically, increased TGF β signaling was also shown in the kinase-deficient T β RII transgenic mice (Denton et al. 2003).

Conclusion

Recent genetic studies of MFS, both in mice and humans, revealed that TGF β signaling is involved in the

pathogenesis of MFS and related disorders. *FBN1* abnormalities appear to be the major genetic cause of MFS, but not the only cause.

MFS-related disorders share many features with MFS. Clinical data should be carefully evaluated, with the recognition that incomplete data might lead to different diagnoses. Further studies are needed in order to establish frames of nosology for MFS and MFS-related disorders, by collection and analysis of extensive genetic and clinical data from many affected patients. An appropriate diagnostic system(s) is needed to differentiate MFS and MFS-related disorders.

Acknowledgment We thank Dr. Remco Visser at the Department of Pediatrics, Leiden University Medical Center, Leiden, The Netherlands, for his critical reading of this manuscript.

References

- Ades LC, Holman KJ, Brett MS, Edwards MJ, Bennetts B (2004) Ectopia lentis phenotypes and the *FBN1* gene. *Am J Med Genet A* 126:284–289
- Ades LC, Sullivan K, Biggin A, Haan EA, Brett M, Holman KJ, Dixon J, Robertson S, Holmes AD, Rogers J, Bennetts B (2006) *FBN1*, *TGFBR1*, and the Marfan-craniosynostosis/mental retardation disorders revisited. *Am J Med Genet A* 140:1047–1058
- Alvarez J, Serra R (2004) Unique and redundant roles of Smad3 in TGF-beta-mediated regulation of long bone development in organ culture. *Dev Dyn* 230:685–699
- Annes JP, Munger JS, Rifkin DB (2003) Making sense of latent TGFbeta activation. *J Cell Sci* 116:217–224
- Arbustini E, Grasso M, Ansaloni S, Malattia C, Pilotto A, Porcu E, Disabella E, Marziliano N, Pisani A, Lanzarini L, Mannarino S, Larizza D, Mosconi M, Antoniazzi E, Zoia MC, Meloni G, Magrassi L, Brega A, Bedeschi MF, Torrente I, Mari F, Tavazzi L (2005) Identification of sixty-two novel and twelve known *FBN1* mutations in eighty-one unrelated probands with Marfan syndrome and other fibrillinopathies. *Hum Mutat* 26:494
- Biggin A, Holman K, Brett M, Bennetts B, Ades L (2004) Detection of thirty novel *FBN1* mutations in patients with Marfan syndrome or a related fibrillinopathy. *Hum Mutat* 23:99
- Boileau C, Jondeau G, Babron MC, Coulon M, Alexandre JA, Sakai L, Melki J, Delorme G, Dubourg O, Bonaiti-Pellie C, et al (1993) Autosomal dominant Marfan-like connective-tissue disorder with aortic dilation and skeletal anomalies not linked to the fibrillin genes. *Am J Hum Genet* 53:46–54
- Boileau C, Jondeau G, Mizuguchi T, Matsumoto N (2005) Molecular genetics of Marfan syndrome. *Curr Opin Cardiol* 20:194–200
- Charbonneau NL, Ono RN, Corson GM, Keene DR, Sakai LY (2004) Fine tuning of growth factor signals depends on fibrillin microfibril networks. *Birth Defects Res C Embryo Today* 72:37–50
- Cohen MM Jr (2003) TGF beta/Smad signaling system and its pathologic correlates. *Am J Med Genet A* 116:1–10
- Collod G, Babron MC, Jondeau G, Coulon M, Weissenbach J, Dubourg O, Bourdarias JP, Bonaiti-Pellie C, Junien C, Boileau C (1994) A second locus for Marfan syndrome maps to chromosome 3p24.2-p25. *Nat Genet* 8:264–268

- Colod-Beroud G, Le Bourdelles S, Ades L, Ala-Kokko L, Booms P, Boxer M, Child A, Comeglio P, De Paepe A, Hyland JC, Holman K, Kaitila I, Loeys B, Matyas G, Nuytink L, Peltonen L, Rantamaki T, Robinson P, Steinmann B, Junien C, Beroud C, Boileau C (2003) Update of the UMD-FBN1 mutation database and creation of an FBN1 polymorphism database. *Hum Mutat* 22:199–208
- Comeglio P, Evans AL, Brice G, Cooling RJ, Child AH (2002) Identification of FBN1 gene mutations in patients with ectopia lentis and marfanoid habitus. *Br J Ophthalmol* 86:1359–1362
- Corson GM, Chalberg SC, Dietz HC, Charbonneau NL, Sakai LY (1993) Fibrillin binds calcium and is coded by cDNAs that reveal a multidomain structure and alternatively spliced exons at the 5' end. *Genomics* 17:476–484
- De Paepe A, Devereux RB, Dietz HC, Hennekam RC, Pyeritz RE (1996) Revised diagnostic criteria for the Marfan syndrome. *Am J Med Genet* 62:417–426
- Denton CP, Zheng B, Evans LA, Shi-wen X, Ong VH, Fisher I, Lazaridis K, Abraham DJ, Black CM, de Crombrughe B (2003) Fibroblast-specific expression of a kinase-deficient type II transforming growth factor beta (TGFbeta) receptor leads to paradoxical activation of TGFbeta signaling pathways with fibrosis in transgenic mice. *J Biol Chem* 278:25109–25119
- Derynck R, Akhurst RJ, Balmain A (2001) TGF-beta signaling in tumor suppression and cancer progression. *Nat Genet* 29:117–129
- Dietz HC, Cutting GR, Pyeritz RE, Maslen CL, Sakai LY, Corson GM, Puffenberger EG, Hamosh A, Nanthakumar EJ, Currstin SM, et al (1991) Marfan syndrome caused by a recurrent de novo missense mutation in the fibrillin gene. *Nature* 352:337–339
- Dietz HC, McIntosh I, Sakai LY, Corson GM, Chalberg SC, Pyeritz RE, Francomano CA (1993) Four novel FBN1 mutations: significance for mutant transcript level and EGF-like domain calcium binding in the pathogenesis of Marfan syndrome. *Genomics* 17:468–475
- Dietz H, Francke U, Furthmayr H, Francomano C, De Paepe A, Devereux R, Ramirez F, Pyeritz R (1995) The question of heterogeneity in Marfan syndrome. *Nat Genet* 9:228–229
- Disabella E, Grasso M, Marziliano N, Ansaldo S, Lucchelli C, Porcu E, Tagliani M, Pilotto A, Diegoli M, Lanzarini L, Malattia C, Pelliccia A, Ficcadenti A, Gabrielli O, Arbustini E (2006) Two novel and one known mutation of the TGFBR2 gene in Marfan syndrome not associated with FBN1 gene defects. *Eur J Hum Genet* 14:34–38
- Downing AK, Knott V, Werner JM, Cardy CM, Campbell ID, Handford PA (1996) Solution structure of a pair of calcium-binding epidermal growth factor-like domains: implications for the Marfan syndrome and other genetic disorders. *Cell* 85:597–605
- Faivre L, Gorlin RJ, Wirtz MK, Godfrey M, Dagonneau N, Samples JR, Le Merrer M, Colod-Beroud G, Boileau C, Munnich A, Cormier-Daire V (2003) In frame fibrillin-1 gene deletion in autosomal dominant Weill-Marchesani syndrome. *J Med Genet* 40:34–36
- Francke U, Berg MA, Tynan K, Brenn T, Liu W, Aoyama T, Gasner C, Miller DC, Furthmayr H (1995) A Gly1127Ser mutation in an EGF-like domain of the fibrillin-1 gene is a risk factor for ascending aortic aneurysm and dissection. *Am J Hum Genet* 56:1287–1296
- Furlong J, Kurczynski TW, Hennessy JR (1987) New Marfanoid syndrome with craniosynostosis. *Am J Med Genet* 26:599–604
- Gilchrist DM (1994) Marfan syndrome or Marfan-like connective-tissue disorder. *Am J Hum Genet* 54:553–554
- Guo D, Hasham S, Kuang SQ, Vaughan CJ, Boerwinkle E, Chen H, Abuelo D, Dietz HC, Basson CT, Shete SS, Milewicz DM (2001) Familial thoracic aortic aneurysms and dissections: genetic heterogeneity with a major locus mapping to 5q13–14. *Circulation* 103:2461–2468
- Habashi JP, Judge DP, Holm TM, Cohn RD, Loeys BL, Cooper TK, Myers L, Klein EC, Liu G, Calvi C, Podowski M, Neptune ER, Halushka MK, Bedja D, Gabrielson K, Rifkin DB, Carta L, Ramirez F, Huso DL, Dietz HC (2006) Losartan, an AT1 antagonist, prevents aortic aneurysm in a mouse model of Marfan syndrome. *Science* 312:117–121
- Halliday DJ, Hutchinson S, Lonie L, Hurst JA, Firth H, Handford PA, Wordsworth P (2002) Twelve novel FBN1 mutations in Marfan syndrome and Marfan related phenotypes test the feasibility of FBN1 mutation testing in clinical practice. *J Med Genet* 39:589–593
- Hasham SN, Willing MC, Guo DC, Mullenburg A, He R, Tran VT, Scherer SE, Shete SS, Milewicz DM (2003) Mapping a locus for familial thoracic aortic aneurysms and dissections (TAAD2) to 3p24–25. *Circulation* 107:3184–3190
- Hutchinson S, Furger A, Halliday D, Judge DP, Jefferson A, Dietz HC, Firth H, Handford PA (2003) Allelic variation in normal human FBN1 expression in a family with Marfan syndrome: a potential modifier of phenotype? *Hum Mol Genet* 12:2269–2276
- Ignotz RA, Massague J (1986) Transforming growth factor-beta stimulates the expression of fibronectin and collagen and their incorporation into the extracellular matrix. *J Biol Chem* 261:4337–4345
- Isogai Z, Ono RN, Ushiro S, Keene DR, Chen Y, Mazzieri R, Charbonneau NL, Reinhardt DP, Rifkin DB, Sakai LY (2003) Latent transforming growth factor beta-binding protein 1 interacts with fibrillin and is a microfibril-associated protein. *J Biol Chem* 278:2750–2757
- Janssens K, ten Dijke P, Ralston SH, Bergmann C, Van Hul W (2003) Transforming growth factor-beta 1 mutations in Camurati-Engelmann disease lead to increased signaling by altering either activation or secretion of the mutant protein. *J Biol Chem* 278:7718–7724
- Jones KB, Myers L, Judge DP, Kirby PA, Dietz HC, Sponseller PD (2005) Toward an understanding of dural ectasia: a light microscopy study in a murine model of Marfan syndrome. *Spine* 30:291–293
- Judge DP, Biery NJ, Keene DR, Geubtner J, Myers L, Huso DL, Sakai LY, Dietz HC (2004) Evidence for a critical contribution of haploinsufficiency in the complex pathogenesis of Marfan syndrome. *J Clin Invest* 114:172–181
- Kaartinen V, Warburton D (2003) Fibrillin controls TGF-beta activation. *Nat Genet* 33:331–332
- Kainulainen K, Karttunen L, Puhakka L, Sakai L, Peltonen L (1994) Mutations in the fibrillin gene responsible for dominant ectopia lentis and neonatal Marfan syndrome. *Nat Genet* 6:64–69
- Katzke S, Booms P, Tiecke F, Palz M, Pletschacher A, Turkmen S, Neumann LM, Pregla R, Leitner C, Schramm C, Lorenz P, Hagemeyer C, Fuchs J, Skovby F, Rosenberg T, Robinson PN (2002) TGGE screening of the entire FBN1 coding sequence in 126 individuals with Marfan syndrome and related fibrillinopathies. *Hum Mutat* 20:197–208
- Ki CS, Jin DK, Chang SH, Kim JE, Kim JW, Park BK, Choi JH, Park IS, Yoo HW (2005) Identification of a novel TGFBR2 gene mutation in a Korean patient with Loeys-Dietz aortic aneurysm syndrome; no mutation in TGFBR2 gene in 30

- patients with classic Marfan's syndrome. *Clin Genet* 68:561–563
- Kielty CM, Sherratt MJ, Shuttleworth CA (2002) Elastic fibres. *J Cell Sci* 115:2817–2828
- Kinoshita A, Saito T, Tomita H, Makita Y, Yoshida K, Ghadami M, Yamada K, Kondo S, Ikegawa S, Nishimura G, Fukushima Y, Nakagomi T, Saito H, Sugimoto T, Kamegaya M, Hisa K, Murray JC, Taniguchi N, Niikawa N, Yoshiura K (2000) Domain-specific mutations in TGFB1 result in Camurati-Engelmann disease. *Nat Genet* 26:19–20
- Kosaki K, Takahashi D, Uda T, Kosaki R, Matsumoto M, Ibe S, Isoe T, Tanaka Y, Takahashi T (2006) Molecular pathology of Shprintzen-Goldberg syndrome. *Am J Med Genet A* 140:104–108; author reply 109–110
- Law C, Bunyan D, Castle B, Day L, Keeton B, Simpson I, Westwood G (2005) Clinical findings in a large family with a predisposition to aortic dilatation and dissection and an R460H mutation in TGFB2. *J Med Genet* 42 [Suppl 1]:S31
- Law CJ, Bunyan D, Castle B, Day L, Simpson I, Westwood G, Keeton B (2006) Clinical features in a family with a R460H mutation in TGFB2. *J Med Genet* (in press)
- Lee B, Godfrey M, Vitale E, Hori H, Mattei MG, Sarfarazi M, Tsiouras P, Ramirez F, Hollister DW (1991) Linkage of Marfan syndrome and a phenotypically related disorder to two different fibrillin genes. *Nature* 352:330–334
- Loeys B, Nuytinck L, Delvaux I, De Bie S, De Paepe A (2001) Genotype and phenotype analysis of 171 patients referred for molecular study of the fibrillin-1 gene FBN1 because of suspected Marfan syndrome. *Arch Intern Med* 161:2447–2454
- Loeys B, De Backer J, Van Acker P, Wettinck K, Pals G, Nuytinck L, Coucke P, De Paepe A (2004) Comprehensive molecular screening of the FBN1 gene favors locus homogeneity of classical Marfan syndrome. *Hum Mutat* 24:140–146
- Loeys BL, Chen J, Neptune ER, Judge DP, Podowski M, Holm T, Meyers J, Leitch CC, Katsanis N, Sharifi N, Xu FL, Myers LA, Spevak PJ, Cameron DE, De Backer J, Hellemans J, Chen Y, Davis EC, Webb CL, Kress W, Coucke P, Rifkin DB, De Paepe AM, Dietz HC (2005) A syndrome of altered cardiovascular, craniofacial, neurocognitive and skeletal development caused by mutations in TGFB1 or TGFB2. *Nat Genet* 37:275–281
- Loeys BL, Schwarze U, Holm T, Callewaert BL, Thomas GH, Pannu H, De Backer JF, Oswald GL, Symoens S, Manouvrier S, Roberts AE, Faravali F, Greco MA, Pyeritz RE, Milewicz DM, Coucke PJ, Cameron DE, Braverman AC, Byers PH, De Paepe AM, Dietz HC (2006) Aneurysm syndromes caused by mutations in the TGF-beta receptor. *N Engl J Med* 355:788–798
- Massague J, Blain SW, Lo RS (2000) TGFbeta signaling in growth control, cancer, and heritable disorders. *Cell* 103:295–309
- Matyas G, Arnold E, Carrel T, Baumgartner D, Boileau C, Berer W, Steinmann B (2006) Identification and in silico analyses of novel TGFB1 and TGFB2 mutations in Marfan syndrome-related disorders. *Hum Mutat* 27:760–769
- Milewicz DM, Michael K, Fisher N, Coselli JS, Markello T, Biddinger A (1996) Fibrillin-1 (FBN1) mutations in patients with thoracic aortic aneurysms. *Circulation* 94:2708–2711
- Mizuguchi T, Colod-Beroud G, Akiyama T, Abifadel M, Harada N, Morisaki T, Allard D, Varret M, Claustres M, Morisaki H, Ihara M, Kinoshita A, Yoshiura K, Junien C, Kajii T, Jondeau G, Ohta T, Kishino T, Furukawa Y, Nakamura Y, Niikawa N, Boileau C, Matsumoto N (2004) Heterozygous TGFB2 mutations in Marfan syndrome. *Nat Genet* 36:855–860
- Neptune ER, Frischmeyer PA, Arking DE, Myers L, Bunton TE, Gayraud B, Ramirez F, Sakai LY, Dietz HC (2003) Dysregulation of TGF-beta activation contributes to pathogenesis in Marfan syndrome. *Nat Genet* 33:407–411
- Ng CM, Cheng A, Myers LA, Martinez-Murillo F, Jie C, Bedja D, Gabrielson KL, Hausladen JM, Mecham RP, Judge DP, Dietz HC (2004) TGF-beta-dependent pathogenesis of mitral valve prolapse in a mouse model of Marfan syndrome. *J Clin Invest* 114:1586–1592
- Pannu H, Fadulu VT, Chang J, Lafont A, Hasham SN, Sparks E, Giampietro PF, Zaleski C, Estrera AL, Safi HJ, Shete S, Willing MC, Raman CS, Milewicz DM (2005a) Mutations in transforming growth factor-beta receptor type II cause familial thoracic aortic aneurysms and dissections. *Circulation* 112:513–520
- Pannu H, Tran-Fadulu V, Milewicz DM (2005b) Genetic basis of thoracic aortic aneurysms and aortic dissections. *Am J Med Genet C Semin Med Genet* 139:10–16
- Pereira L, Andrikopoulos K, Tian J, Lee SY, Keene DR, Ono R, Reinhardt DP, Sakai LY, Biery NJ, Bunton T, Dietz HC, Ramirez F (1997) Targeting of the gene encoding fibrillin-1 recapitulates the vascular aspect of Marfan syndrome. *Nat Genet* 17:218–222
- Pereira L, Lee SY, Gayraud B, Andrikopoulos K, Shapiro SD, Bunton T, Biery NJ, Dietz HC, Sakai LY, Ramirez F (1999) Pathogenetic sequence for aneurysm revealed in mice underexpressing fibrillin-1. *Proc Natl Acad Sci U S A* 96:3819–3823
- Ramirez F, Sakai LY, Dietz HC, Rifkin DB (2004) Fibrillin microfibrils: multipurpose extracellular networks in organismal physiology. *Physiol Genomics* 19:151–154
- Rifkin DB (2005) Latent transforming growth factor-beta (TGF-beta) binding proteins: orchestrators of TGF-beta availability. *J Biol Chem* 280:7409–7412
- Robinson PN, Godfrey M (2000) The molecular genetics of Marfan syndrome and related microfibrilopathies. *J Med Genet* 37:9–25
- Robinson PN, Neumann LM, Demuth S, Enders H, Jung U, Konig R, Mitulla B, Muller D, Muschke P, Pfeiffer L, Prager B, Somer M, Tinschert S (2005) Shprintzen-Goldberg syndrome: fourteen new patients and a clinical analysis. *Am J Med Genet A* 135:251–262
- Robinson P, Neumann L, Tinschert S (2006) Response to Kosaki et al. "Molecular pathology of Shprintzen-Goldberg syndrome". *Am J Med Genet* 140A:109–110
- Rommel K, Karck M, Haverich A, Schmidtke J, Arslan-Kirchner M (2002) Mutation screening of the fibrillin-1 (FBN1) gene in 76 unrelated patients with Marfan syndrome or Marfanoid features leads to the identification of 11 novel and three previously reported mutations. *Hum Mutat* 20:406–407
- Rommel K, Karck M, Haverich A, von Kodolitsch Y, Rybczynski M, Muller G, Singh KK, Schmidtke J, Arslan-Kirchner M (2005) Identification of 29 novel and nine recurrent fibrillin-1 (FBN1) mutations and genotype-phenotype correlations in 76 patients with Marfan syndrome. *Hum Mutat* 26:529–539
- Sakai H, Visser R, Ikegawa S, Ito E, Numabe H, Watanabe Y, Mikami H, Kondoh T, Kitoh H, Sugiyama R, Okamoto N, Ogata T, Fodde R, Mizuno S, Takamura K, Egashira M, Sasaki N, Watanabe S, Nishimaki S, Takada F, Nagai T, Okada Y, Aoka Y, Yasuda K, Iwasa M, Kogaki S, Harada N, Mizuguchi T, Matsumoto N (2006) Comprehensive genetic analysis of relevant four genes in 49 patients with

- Marfan syndrome or Marfan-related phenotypes. *Am J Med Genet A* 140:1719–1725
- Schrijver I, Liu W, Odom R, Brenn T, Oefner P, Furthmayr H, Francke U (2002) Premature termination mutations in *FBN1*: distinct effects on differential allelic expression and on protein and clinical phenotypes. *Am J Hum Genet* 71:223–237
- Serra R, Karaplis A, Sohn P (1999) Parathyroid hormone-related peptide (PTHrP)-dependent and -independent effects of transforming growth factor beta (TGF-beta) on endochondral bone formation. *J Cell Biol* 145:783–794
- Singh KK, Rommel K, Mishra A, Karck M, Haverich A, Schmidtke J, Arslan-Kirchner M (2006) *TGFBR1* and *TGFBR2* mutations in patients with features of Marfan syndrome and Loeys–Dietz syndrome. *Hum Mutat* 27: 770–777
- Sood S, Eldadah ZA, Krause WL, McIntosh I, Dietz HC (1996) Mutation in fibrillin-1 and the Marfanoid-craniosynostosis (Shprintzen–Goldberg) syndrome. *Nat Genet* 12:209–211
- ten Dijke P, Miyazono K, Heldin CH (1996) Signaling via hetero-oligomeric complexes of type I and type II serine/threonine kinase receptors. *Curr Opin Cell Biol* 8:139–145
- Tynan K, Comeau K, Pearson M, Wilgenbus P, Levitt D, Gasner C, Berg MA, Miller DC, Francke U (1993) Mutation screening of complete fibrillin-1 coding sequence: report of five new mutations, including two in 8-cysteine domains. *Hum Mol Genet* 2:1813–1821
- Vaughan CJ, Casey M, He J, Veugelers M, Henderson K, Guo D, Campagna R, Roman MJ, Milewicz DM, Devereux RB, Basson CT (2001) Identification of a chromosome 11q23.2–q24 locus for familial aortic aneurysm disease, a genetically heterogeneous disorder. *Circulation* 103:2469–2475
- Wieser R, Wrana JL, Massague J (1995) GS domain mutations that constitutively activate T beta R-I, the downstream signaling component in the TGF-beta receptor complex. *EMBO J* 14:2199–2208
- Wrana JL, Attisano L, Wieser R, Ventura F, Massague J (1994) Mechanism of activation of the TGF-beta receptor. *Nature* 370:341–347

Role of DNA Methylation and Histone H3 Lysine 27 Methylation in Tissue-Specific Imprinting of Mouse *Grb10*⁷

Yoko Yamasaki-Ishizaki,^{1,2,8} Tomohiko Kayashima,¹ Christophe K. Mapendano,¹ Hidenobu Soejima,³
Tohru Ohta,^{4,5} Hideaki Masuzaki,² Akira Kinoshita,^{1,8} Takeshi Urano,⁵ Ko-ichiro Yoshiura,^{1,8}
Naomichi Matsumoto,⁶ Tadayuki Ishimaru,² Tsunehiro Mukai,³
Norio Niikawa,^{1,8} and Tatsuya Kishino^{7,8*}

Departments of Human Genetics¹ and Obstetrics and Gynecology,² Graduate School of Biomedical Sciences, Nagasaki University, Nagasaki, Japan; Department of Biomolecular Sciences, Saga University, Saga, Japan³; The Research Institute of Personalized Health Sciences, Health Sciences University of Hokkaido, Hokkaido, Japan⁴; Department of Biochemistry II, Graduate School of Medicine, Nagoya University, Nagoya, Japan⁵; Department of Human Genetics, Graduate School of Medicine, Yokohama City University, Yokohama, Japan⁶; Division of Functional Genomics, Center for Frontier Life Sciences, Nagasaki University, Nagasaki, Japan⁷; and CREST, Japan Science and Technology Agency, Kawaguchi, Japan⁸

Received 19 July 2006/Accepted 24 October 2006

Mouse *Grb10* is a tissue-specific imprinted gene with promoter-specific expression. In most tissues, *Grb10* is expressed exclusively from the major-type promoter of the maternal allele, whereas in the brain, it is expressed predominantly from the brain type promoter of the paternal allele. Such reciprocally imprinted expression in the brain and other tissues is thought to be regulated by DNA methylation and the Polycomb group (PcG) protein Eed. To investigate how DNA methylation and chromatin remodeling by PcG proteins coordinate tissue-specific imprinting of *Grb10*, we analyzed epigenetic modifications associated with *Grb10* expression in cultured brain cells. Reverse transcriptase PCR analysis revealed that the imprinted paternal expression of *Grb10* in the brain implied neuron-specific and developmental stage-specific expression from the paternal brain type promoter, whereas in glial cells and fibroblasts, *Grb10* was reciprocally expressed from the maternal major-type promoter. The cell-specific imprinted expression was not directly related to allele-specific DNA methylation in the promoters because the major-type promoter remained biallelically hypomethylated regardless of its activity, whereas gametic DNA methylation in the brain type promoter was maintained during differentiation. Histone modification analysis showed that allelic methylation of histone H3 lysine 4 and H3 lysine 9 were associated with gametic DNA methylation in the brain type promoter, whereas that of H3 lysine 27 regulated by the Eed PcG complex was detected in the paternal major-type promoter, corresponding to its allele-specific silencing. Here, we propose a molecular model that gametic DNA methylation and chromatin remodeling by PcG proteins during cell differentiation cause tissue-specific imprinting in embryonic tissues.

Genomic imprinting in mammals describes the situation where there is non-equivalence in expression between the maternal and paternal alleles at certain gene loci, depending on the parental origin. Genomic imprinting plays essential roles in development, growth, and behavior (6, 30, 31). Such parental origin-specific gene regulation is caused by epigenetic modifications that occur during gametogenesis without any nucleic acid changes. One of the well-known epigenetic modifications is DNA methylation. In the imprinted loci, differentially methylated regions between the maternal and paternal alleles are often found and associated with parental allele-specific expression (7). Another well-known epigenetic modification is histone modification, which represents the determinant of epigenetic features associated with imprinted genes. It has been reported that parental origin-specific gene expression on some imprinted genes is determined by DNA methylation and/or histone modifications (12, 13, 16, 23, 29, 40). Polycomb group

(PcG) proteins also play an important role in various epigenetic phenomena (3), such as maintaining the silent state of the homeotic genes, maintaining X-chromosome inactivation (36), and silencing imprinted genes in mammals (24, 33). PcG protein complexes are thought to maintain long-term gene silencing during development through alterations of local chromatin structure (3, 27).

Mouse *Grb10* encoding the growth factor receptor-bound protein 10 (Grb10) is an imprinted gene with tissue-specific and promoter-specific expression. In most tissues, the major-type transcript of *Grb10* is expressed exclusively from the major-type promoter of the maternal allele, whereas in the brain, the brain type transcript is expressed predominantly from the brain type promoter of the paternal allele (1, 17). DNA methylation analysis has revealed that the CpG island (CGI) in the brain type promoter (CGI2) was gametically methylated in the oocyte as a primary imprint and remained methylated exclusively on the maternal allele in somatic tissues, while the CpG island in the major-type promoter (CGI1) was biallelically hypomethylated in somatic tissues (see Fig. 1 and 4) (17). Hikichi et al. proposed the model for tissue-specific imprinting of *Grb10* that the major-type transcript is regulated by DNA methylation-sensitive insulator (CTCF) binding in CGI2 and

* Corresponding author. Mailing address: Division of Functional Genomics, Center for Frontier Life Sciences, Nagasaki University, Sakamoto 1-12-4, Nagasaki 852-8523, Japan. Phone: 81-95-849-7120. Fax: 81-95-849-7178. E-mail: kishino@net.nagasaki-u.ac.jp.

⁷ Published ahead of print on 13 November 2006.

the brain type transcript is regulated by putative brain-specific activators (17). They suggested that allelic DNA methylation in CGI2 can orchestrate reciprocal imprinting of the two promoters of the *Grb10* gene. This model was partially supported by the imprinting analysis of knockout mice of the *Dnmt3L* gene, encoding a factor for acquisition of maternal methylation imprint in germ cells (14, 18). In the embryos (*Dnmt3L^{m-/-}*), produced from *Dnmt3L^{-/-}* females, maternal chromosome-specific DNA methylation in CGI2 was lost and null expression of the major-type transcript was detected (2). Recently, the PcG protein Eed (embryonic ectoderm development) was identified as a member of a new class of *trans*-acting factors, which regulate the expression of some paternally repressed imprinted genes, *Cdkn1c*, *Ascl2*, *Meg3*, and *Grb10* (24). In *Eed^{-/-}* embryos, the major-type transcript of *Grb10* was biallelically expressed from the major-type promoter without major alteration of DNA methylation in gametically methylated CGI2, albeit various hypomethylated patterns were observed on the paternal allele (24). The expression analysis of these knockout mice suggests that DNA methylation and chromatin remodeling by PcG proteins represent the epigenetic factors that are necessary for establishing and/or maintaining the imprinted expression of *Grb10*. It remains unknown how they coordinate the tissue-specific and promoter-specific imprinting of *Grb10*.

Recently, mouse genes with brain-specific imprinting patterns were reported. They are *Ube3a* and *Murr1*, with neuron-specific and brain developmental stage-specific expressions, respectively. *Ube3a* is biallelically expressed in most tissues but expressed exclusively from the maternal allele only in neurons, leading to apparent partial imprinting with predominant maternal *Ube3a* expression in the whole brain (38). *Murr1* is imprinted in the adult brain, especially in mature neurons, but not in embryonic and neonatal brains (37). These lines of evidence suggest that brain-specific imprinting may be regulated in part by epigenetic modifications, depending on specification and maturation of cell lineages in the developing brain (9, 19).

Since *Grb10* is a tissue-specific imprinted gene, we hypothesized that tissue-specific reciprocal imprinting of *Grb10* also depends on cell-specific epigenetic modifications acquired during cell differentiation. To examine our hypothesis, we performed an epigenetic analysis of brain cells with the aid of primary cortical cell cultures, in which neurons or glial cells were cultured separately from products of reciprocal crosses between the C57BL/6 and PWK strains (divergent strains of *Mus musculus*). In each cultured brain cell, *Grb10* expression and epigenetic factors such as DNA methylation and histone modifications were analyzed to investigate how DNA methylation and chromatin remodeling by PcG proteins establish and maintain the tissue-specific and promoter-specific imprinting of *Grb10*.

MATERIALS AND METHODS

Mice. All procedures were performed with approval from the Nagasaki University Institutional Animal Care and Use Committee. F₁ hybrid mice were obtained by mating C57BL/6 females with PWK males [(C57BL/6 × PWK)F₁] and vice versa [(PWK × C57BL/6)F₁]. Telencephalon/cerebral cortices and embryonic fibroblasts were prepared from embryonic day 10 (E10) to E15. Tissues were used for RNA and DNA extraction or primary cultures. Brain tissue

for reverse transcriptase (RT) PCR was dissected at E10, E16, postnatal day 1, postnatal day 5, 2 weeks, 4 weeks, 6 weeks, and 14 months.

Primary culture. Methods of primary cultures of cortical neurons, glial cells, and embryonic fibroblasts have been described elsewhere (38). In brief, E15 cerebral cortices without meninges were trypsinized to dissociate brain cells. For neuronal culture, dissociated cells were cultured in neurobasal medium (Gibco BRL, Carlsbad, CA) with B27 supplement (Gibco BRL). Cultures were maintained in 5% CO₂ at 37°C for 5 days. For the long culture, half of the culture medium was changed every 3 to 4 days. For glial cell culture, dissociated brain cells were cultured overnight in Dulbecco's modified Eagle's medium (Sigma, St. Louis, MO) supplemented with 10% fetal calf serum, and then the medium was changed to Neurobasal medium (Gibco BRL) with G5 supplement (GIBCO BRL). After 5 to 7 days in the primary culture, cultured glial components were subcultured. Cultures were maintained in 5% CO₂ at 37°C for a total of 14 days. For embryonic fibroblast culture, embryonic fibroblasts derived from E15 embryonic skin were cultured in Dulbecco's modified Eagle's medium supplemented with 10% fetal calf serum.

cDNA synthesis. Total RNA was isolated from cultured cells and tissues with RNeasy (QIAGEN, Hilden, Germany) according to the manufacturer's protocol. The RNA was treated with amplification grade DNase I (Invitrogen, Carlsbad, CA) to degrade any genomic DNA present in the sample. The cDNA was generated from total RNA by SuperScript II reverse transcriptase (Invitrogen) primed with oligo(dT)₁₂₋₁₈ primers. The first-strand cDNA was synthesized at 42°C for 50 min. Then, mRNA-cDNA chains were denatured and the reverse transcriptase activity was arrested by heating at 70°C for 15 min. An identical reaction was carried out without reverse transcriptase as a negative control.

RT-PCR for expression analysis. The cDNA obtained was used to perform RT-PCR for expression analysis. The expression of each *Grb10* transcript was analyzed using primers 1aF and 1R for the major-type transcript and using primers 1bF and 1R for the brain type transcript. Other transcripts, including exon 1c, were amplified by primer sets 1cF/e2R and 1aF/1cR. PCR amplification with primers 1aF and 1R was performed for 32 to 35 cycles of 15 s at 96°C, 20 s at 60°C, and 60 s at 72°C, with primers 1bF and 1R for 32 to 38 cycles of 15 s at 96°C, 20 s at 60°C, and 60 s at 72°C, and with primer sets 1cF/e2R and 1aF/1cR for 35 cycles of 15 s at 96°C, 20 s at 60°C, and 60 s at 72°C. The primers for *Map2*, *Gfap*, and *Gapdh* used for evaluation of the cultured cells have been described elsewhere (38). For a semiquantitative RT-PCR, optimal template cDNA concentrations were determined according to *Gapdh* amplification. PCR products were amplified for 25 to 30 cycles of 15 s at 96°C, 20 s at 55°C, and 30 s at 72°C.

Quantitative analysis of gene expression by real-time PCR. cDNA was applied to real-time PCR for quantitative analysis of each transcript using SYBR green and an ABI Prism 7900 (PE Applied Biosystems, Foster City, CA). PCR was performed on samples at least in triplicate according to the manufacturer's protocol to control for PCR variation. To standardize each experiment, the results were represented as a percentage of expression, calculated by dividing the average value of the expression of the target gene by that of an internal control gene, *Gapdh* (38). The primers used for real-time PCR were primers 1aF and 1R for the major-type transcript and primers Q-1bF and Q-1bR for the brain type transcript. Each experiment was repeated with independent RNAs two to three times.

Sequencing for allelic differences. A sequence chromatogram was used to detect allelic differences of PCR products. Parental expression of major/brain type transcripts in the brain and kidney was analyzed by RT-PCR using primer sets 1aF/coR and 1bF/coR for 35 to 38 cycles of 15 s at 96°C, 20 s at 60°C, and 120 s at 72°C. Parental chromosome-specific histone modifications in the major-type promoter were analyzed by PCR using the primer set ChIP-F/ChIP-R for 30 cycles of 30 s at 95°C, 30 s at 58°C, and 30 s at 72°C. The PCR products were analyzed by direct sequencing with a BigDye Terminator cycle sequencing kit (PE Applied Biosystems) on an automated sequencer, the ABI Prism 3100 genetic analyzer (PE Applied Biosystems).

DNA methylation analysis. Isolated DNA was treated with sodium bisulfite using a CpGenome DNA modification kit (Chemicon International Inc., Temecula, CA) according to the manufacturer's protocol. Bisulfite-treated DNA samples were subjected to nested PCR amplification using the following first and second primer pairs, respectively, for each CGI: CGI1, Me1F/Me-1R and Me-1F/Me-1R; CGI2, Me-2F/Me-2R and Me-2F/Me-2R; and CGI3, Me-3F/Me-3R and Me-3F/Me-3R. After the first PCR using the first primer set, the products were used as templates for nested PCR using the second primer set. The nested PCR products were cloned into the TA cloning vector (Invitrogen), and at least 32 clones for each sample were sequenced.

ChIP. A chromatin immunoprecipitation (ChIP) assay was performed with a ChIP assay kit (Upstate Biotechnology, Lake Placid, NY) according to the manufacturer's protocol. In brief, the chromatin of cultured cells was prepared from $\sim 1.0 \times 10^6$ cells and treated with formaldehyde to cross-link DNA to

TABLE 1. Primers used in this study

Function(s) and primer	Sequence (5'-3')	Annealing temp (°C) (PCR cycle no.) ^a
Expression and imprinting analysis		
1aF ^b	CACGAAGTTTCCGCGCA	
1bF	GCGATCATTCTCTCTGAGC	
1R ^b	AGTATCAGTATCAGACTGCATGTTG	
1cF	ATCGCCATCTACAGTTTCTG	
1cR	CAAGGTACAGAGCTAGGACG	
e2R	CTGGTTGGCTTCTTTGTTGTGG	
coR	TACGGATCTGCTCATCTTCG	
ChIP-F	TCACTTTAGAAACCGGGCA	
ChIP-R	AAACTCGGGCTTGCTCA	
Quantitative analysis		
Q-1bF	TCATTCGTCTCTGAGCGGCA	
Q-1bR	ATACGTGTTACATGCGCCAA	
Q-ChIP1F	TCACTTTAGAAACCGGGCA	
Q-ChIP1R	AAACTCGGGCTTGCTCA	
Q-ChIP2F	GATCATTCTGCTCTGAGC	
Q-ChIP2R	ATGCGGCAACATGCGCTGACA	
Hot-stop PCR and SSCP analysis		
ChIP2F-1	TCATTCGTCTCTGAGCGGCA	60 (32)
ChIP2R-1	TCTGGAGCCTAGAGGAGCG	
ChIP2F-2	AAGCGGTGCTGGTTTGTGTA	60 (35)
ChIP2R-2	ATACGTGTTACATGCGCCAA	
DNA methylation analysis		
CGI1 1st		53 (35)
Me-1F	TGGGGTTTAATATTAAGTTTGA	
Me-1R	TTACATCTCTTAAATAAAAACA	
CGI1 2nd		53 (35)
Me-1F'	TGGGGTTTAATATTAAGTTTGA	
Me-1R'	AAATCACCTATAACTCTCTCTAC	
CGI2 1st		50 (40)
Me-2F	TGGAGTTTAGAGGAG	
Me-2R	AATAGTTATTTAGTAAGGG	
CGI2 2nd		50 (10)
Me-2F'	TGGAGTTTAGAGGAG	
Me-2R'	TAAGTGAAGTAATATAGTT	
CGI3 1st		53 (40)
Me-3F	AAAGAAGGTTTGGAGAGATTATTT	
Me-3R	CAAACAAAACCTACTATATTTAATTTAAAC	
CGI3 2nd		53 (10)
Me-3F'	AAGGTTTGGAGAGATTATTTTGTATT	
Me-3R'	TAATTTAAACTTAACACTATTAATATACC	

^a For expression and imprinting analysis, the annealing temperature and PCR cycle number depend on the combination of primers used for each analysis. See details in Materials and Methods. For quantitative analysis, the PCR conditions were decided according to the manufacturer's protocol.

^b Also used for quantitative analysis.

protein in situ, sonicated to an average size of 0.5 kb, and immunoprecipitated with antibodies. Antibodies against acetyl histone H3 (H3Ac; catalog no. 06-599), acetyl histone H4 (H4Ac; catalog no. 09-866), Lys4 dimethylated histone H3 (H3meK4; catalog no. 07-030), Lys9 trimethylated H3 (H3me3K9; catalog no. 07-212), and Lys27 trimethylated H3 (H3meK27; catalog no. 07-449) were obtained from Upstate Biotechnology. The monoclonal antibody against Lys9 dimethylated histone H3 (H3me2K9) was developed previously (26). Immunoprecipitated samples without antibodies or with rabbit immunoglobulin G precipitation were used as negative controls for precipitations with specific antibodies in each experiment.

Quantitative analysis of immunoprecipitated DNA by real-time PCR. Immunoprecipitated DNA and input DNA were analyzed by real-time PCR using the same protocol as that used for gene expression analysis. For DNA immunoprecipitated with H3Ac, H4Ac, and H3meK4 antibodies, the quantitative value of immunoprecipitated DNA in each CGI was normalized by dividing the average value of each CGI by that of the internal control, *Gapdh*. For DNA immunoprecipitated with H3me2K9 and H3me3K9 antibodies, the average value of *D13Mit55* was used instead of the value of *Gapdh*. Each normalized value of immunoprecipitated DNA was further divided by the normalized value of the

corresponding input DNA. For the evaluation of DNA immunoprecipitated with H3meK27 antibody, the results were presented as a percentage of immunoprecipitation, calculated by dividing the average value of immunoprecipitated DNA by the average value of the corresponding input DNA. Each experiment was performed three times with independent chromatin extracts. The primers used for real-time PCR were primers Q-ChIP1F and Q-ChIP1R for CGI1 analysis and primers Q-ChIP2F and Q-ChIP2R for CGI2 analysis. The primers for *Gapdh* and *D13Mit55* have been described elsewhere (16).

Hot-stop PCR and SSCP analysis. Hot-stop PCR was performed for the analysis of allele-specific histone modifications as follows. After a number of PCR cycles sufficient to detect a product using primers ChIP2F-1 and ChIP2R-1, primer ChIP2R-1 labeled by [γ -³²P]ATP was added to the mixture, and then one cycle of PCR was performed. The PCR products were digested with the restriction endonuclease Hpy188I and electrophoresed in a 4% polyacrylamide gel. Single-strand conformation polymorphism (SSCP) analysis of PCR products was performed for allele-specific histone methylation in the presence of [γ -³²P]ATP-labeled primers ChIP2F-2 and ChIP2R-2. PCR products were resolved by electrophoresis in an MDE nondenaturing acrylamide gel (FMC BioProduct, Rockland, ME).

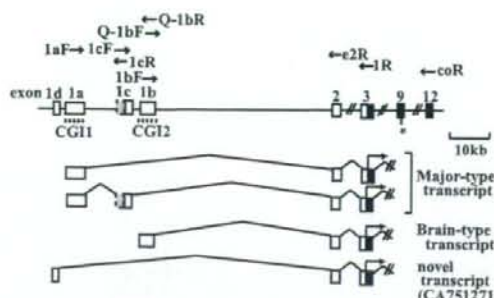


FIG. 1. Tissue-specific transcripts of *Grb10*. Filled boxes, open boxes, and shaded boxes represent protein-coding regions, 5' untranslated regions, and extended exons 1c, respectively. The dashed lines indicate the CpG islands (CG11 and CG12) in the promoters. The primers used for RT-PCR are shown. The asterisk indicates the polymorphic site (G/A) between the C57BL/6 and PWK strains.

Primers. The primers used for the analysis are listed in Table 1.

RESULTS

Mouse *Grb10* has several tissue-specific promoters. Three different promoters of *Grb10* have previously been reported to initiate tissue-specific transcripts (Fig. 1). We first analyzed the expression of each transcript in E16 fetal tissues. The major-type transcript amplified by PCR using primers 1aF and e2R in exons 1a and 2, respectively, was detected in the fetal brain but was less detected in other tissues, while the brain type transcript amplified by primers 1bF and e2R in exons 1b and 2, respectively, was detected exclusively in the fetal brain (Fig. 2A). Another transcript which was previously reported to be brain specific in adult tissues (1) was examined in fetal tissues. PCR using primers 1cF and e2R in exons 1c and 2, respectively, showed that exon 1c was expressed not only in the fetal brain but also in the fetal liver and kidney (Fig. 2A). To assess whether exon 1c is an alternatively spliced exon of the major-type transcript with exon 1a, we performed PCR using primers 1aF and 1cR in exons 1a and 1c, respectively. The PCR product containing exons 1a and 1c was detected in the fetal tissues (Fig. 2A). Sequence analysis of the RT-PCR product revealed that exon 1c was extended 67 bp upstream of the previously published exon 1c with the consensus splicing site (Fig. 1). Any RT-PCR products with both exons 1a and 1b or both exons 1c and 1b were not found (data not shown). Furthermore, we identified another putative exon, 1d, located 1.2 kb upstream of exon 1a in the expressed sequence tag database (GenBank accession no. CA751271). The existence of the novel exon 1d was confirmed by RT-PCR in the embryonic liver but not in other tissues, including the brain (data not shown).

Expression of *Grb10* shifts from the major-type to the brain type transcript during brain development. To confirm whether the expression level of the brain type transcript changes during brain development, the major-type and brain type transcripts arising from exons 1a and 1b, respectively, were quantitatively analyzed at various developmental stages of the brain. Real-time PCR analysis showed that in the brain, the major-type transcript was highly expressed at E10 and decreased accord-

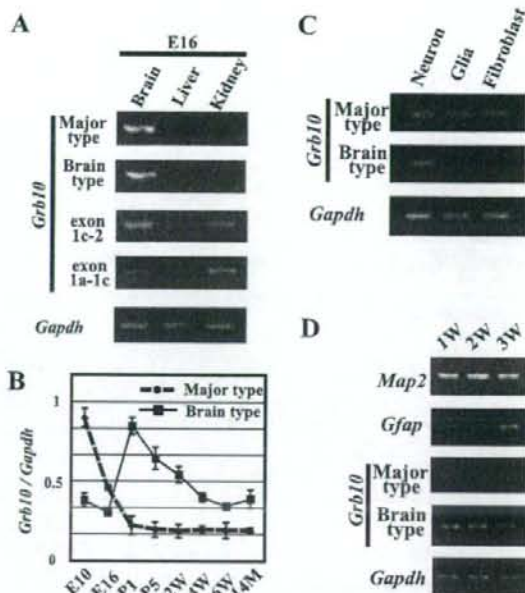


FIG. 2. Expression analysis of each transcript in embryonic tissues by RT-PCR. (A) Semiquantitative analysis of tissues from the E16 embryo. Exon 1c-2 and exon 1a-1c represent RT-PCR products amplified by primer sets 1cF/e2R and 1aF/1cR, respectively. The concentration of each cDNA was adjusted for *Gapdh* amplification as an internal control. (B) Quantitative evaluation of major-type and brain type transcripts in brain tissues from different developmental stages by real-time PCR. The relative amounts of major-type and brain type transcripts are shown. The relative amount of each transcript was calculated by normalizing each value with an internal control, *Gapdh*. Standard errors of the means are indicated by bars. (C) Expression analysis of major-type and brain type transcripts in the primary cell culture. (D) Evaluation of expression of marker genes and each *Grb10* transcript according to the culture period. 1w (1 week), 2w (2 weeks), and 3w (3 weeks) indicate the periods of neuron culture. P1, postnatal day 1; 14M, 14 months.

ing to brain development, while expression of the brain type transcript was high in the perinatal period and gradually decreased thereafter (Fig. 2B). The result indicates that *Grb10* transcripts shift from the major type to the brain type during early brain development.

The brain-specific transcript is expressed in neurons but not in glial cells. Is the brain type transcript expressed exclusively in the brain restricted to the cell type? To know which type of brain cells, neurons or glial cells, express the brain type transcript, expression analysis of cultured neurons and glial cells was carried out. Prior to the analysis, we confirmed by immunostaining and RT-PCR with the brain precursors, neuronal and glial markers, that over 95% of the two cultured cell types were postmitotic neurons and astrocytes, respectively (data not shown). RT-PCR in cultured cells revealed that the major-type transcript was expressed in all cultured brain cells but that the brain type transcript was expressed only in neurons (Fig. 2C). We next tried to investigate whether these transcripts in the brain were associated with the maturation of

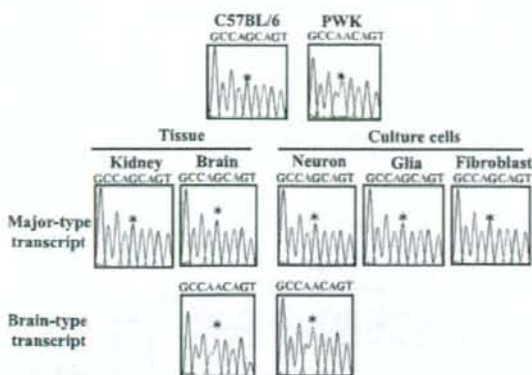


FIG. 3. Imprinting analysis of promoter-specific expression of *Grb10* by sequence chromatograms. Upper panels show the chromatograms of the genomic PCR products from each strain. Middle and lower panels show the chromatograms of the RT-PCR products from tissues and cultured cells of the F_1 hybrid, in which alleles were distinguished by the single-nucleotide (G/A) polymorphism (*) at exon 9.

neurons. Neurons were cultured for 1, 2, and 3 weeks, and semiquantitative RT-PCR was carried out. Before expression analysis of *Grb10*, the status of cell proliferation and differentiation by long culture was evaluated by primers for *Map2* as a marker for neurons and *Gfap* as a marker for astrocytes under the normalization of cDNA concentration to *Gapdh* (Fig. 2D). The expression of *Map2* never changed in 3-week-cultured cells, while that of *Gfap* was detected in the cells cultured for 3 weeks. In these long-culture cells, the brain type transcript was continuously expressed during culture periods, while the major-type transcript was less expressed than the brain type transcript. These results suggest that both types of transcripts are expressed in neurons and that the switching of the promoter from the major type to the brain type is observed during long culture periods.

Promoter-specific paternal expression of *Grb10* in the brain. To investigate the imprinted expression of *Grb10*, we first examined parental expression of the major-type and the brain type transcripts in the brain and kidney from F_1 hybrid mice by direct sequencing of the RT-PCR product. A polymorphic site (G/A) in exon 9 between the C57BL/6 and PWK strains was used to determine the paternal allele (Fig. 1). As previously reported by Hikichi et al. (17), the major-type transcript was expressed exclusively from the maternal allele in the kidney and brain, while the brain type transcript was expressed from the paternal allele only in the brain (Fig. 3). We next examined promoter-specific imprinting in neurons, glial cells, and fibroblasts. Expression of the major-type transcript originated exclusively from the maternal allele in all cultured cells, but that of the brain type transcript detected only in neurons originated from the paternal allele (Fig. 3). Thus, predominant paternal *Grb10* expression in the brain, as previously described, can be explained by a combination of paternally expressed brain type transcript in neurons and maternally expressed major-type transcript in all cells.

Differentially methylated CGI2 is maintained in cultured neurons and glial cells. As we found that the brain type tran-

script was initiated from exon 1b of the paternal allele only in neurons, we analyzed the methylation status of the brain type promoter in neurons and glial cells by the bisulfite method. As shown in Fig. 4A, three promoters are located within different CGIs: exon 1a in CGI1, exon 1b in CGI2, and exon 1c in the "weaker" CpG island, CGI3. The parental origin of the methylated allele was identified by polymorphic sites in F_1 hybrids between the C57BL/6 and PWK strains. The methylation analysis of CGI2 showed that the differential methylation established in the germ cells (1, 17) was maintained in neurons and glial cells (Fig. 4B). That in other CpG islands, CGI1 and CGI3, revealed biallelic hypomethylation and hypermethylation, respectively. CGI1 and CGI3 did not show any differential methylation in the cells, although CGI3 was reported to be a putative differentially methylated region in the mouse brain with uniparental disomy for chromosome 11 (1). The methylation status in CGIs, except CGI3, in cultured cells was consistent with that previously reported for tissues (1, 17).

Parental chromosome-specific histone modifications in CGI2 correlate with allele-specific expression of the brain type transcript in neurons. Parental origin-specific histone modifications are reported to represent the determinant of epigenetic features as well as DNA methylation. Using specific antibodies against acetylated histone H3 (H3Ac), acetylated histone H4 (H4Ac), dimethylated Lys4 histone H3 (H3mK4), and di- and trimethylated Lys9 histone H3 (H3me2K9 and H3me3K9), we performed a ChIP assay with cultured cells. After evaluation of ChIP DNA by allele-specific histone modifications in the *Lit1* promoter region as a control (16), histone modifications in CGI1, CGI2, and CGI3 were analyzed by real-time PCR to quantify their precipitated chromatins in these CGIs. To normalize each value, *Gapdh* and *D13Mit55* were used as internal control sequences, where acetylated and methylated histones were known to be biallelically immunoprecipitated, depending on the corresponding antibodies. In CGI2, where the maternal allele-specific DNA methylation was established in the oocyte, H3Ac, H4Ac, H3mK4, and H3me3K9 were clearly immunoprecipitated in neurons, while in glial cells and fibroblasts, although H3mK4 and H3me3K9 were well immunoprecipitated, H3Ac and H4Ac were less precipitated (Fig. 5A). The results obtained with the antibody against H3me2K9 (data not shown) were similar to those obtained with the antibody against H3me3K9.

To elucidate the parental chromosome-specific histone modifications in CGI2 in neurons, hot-stop PCR was performed (15, 32). The restriction endonuclease Hpy188I was used to recognize the polymorphic site in CGI2. For each of the precipitated samples, the ratio of the paternal to maternal band intensities was determined. These ratios were corrected for the paternal-to-maternal ratios in the input chromatin, because the maternal and paternal alleles were not equally represented in the input chromatin. One of the parental alleles is possibly more sensitive to sonication in these regions because of relaxed chromatin (12, 16, 39). The result revealed that histones H3 and H4 were hyperacetylated and that H3K4 was hypermethylated predominantly on the paternal chromosome (Fig. 5B). To investigate allele-specific histone trimethylation of H3K9 in neurons and fibroblasts, SSCP analysis of PCR products was also performed. In

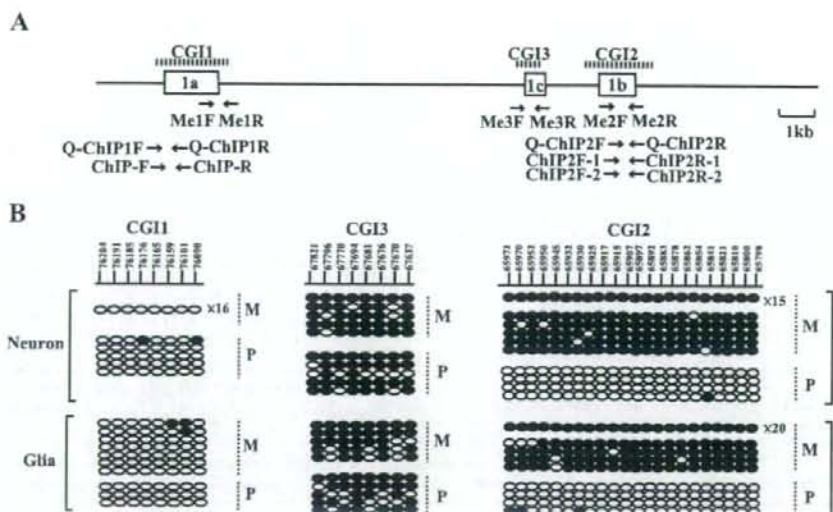


FIG. 4. Methylation status of CpG islands in neurons and glial cells. (A) Schematic structure of CpG islands. The dashed lines indicate the registered regions of CGI1, CGI2, and CGI3 (1, 17). Open boxes and arrows represent exons and primers used for methylation analysis and ChIP analysis, respectively. (B) Allele-specific DNA methylation analysis of cultured cells by bisulfite PCR and sequencing. Numbers on the line in the upper panel represent nucleotide positions, given according to GenBank accession no. AL663087. Each line shows an individual clone, and each oval represents a CpG nucleoside: the filled and open ovals indicate hypermethylated and hypomethylated CpGs, respectively. The numbers with "x" given at the right end of the clone lines represent the number of individual clones that show the same pattern of DNA methylation. Parental alleles (M, maternal; P, paternal) are distinguished by DNA polymorphisms between the C57BL/6 and PWK strains.

neurons and fibroblasts, H3K9 was hypermethylated on the maternal chromosome (Fig. 5C).

Parental chromosome-specific methylation of histone H3K27 but not H3K9 in CGI1 correlates with allele-specific expression of the major-type transcript. Histone modifications in CGI1, where CpGs were biallelically hypomethylated in tissues and cultured cells, were next analyzed. In CGI1, H3Ac, H4Ac, and H3mK4 were clearly precipitated in glial cells and fibroblasts, while the precipitations were not observed in neurons (Fig. 5A). H3me3K9 and H3me2K9 in CGI1 were not precipitated in neurons and glial cells (Fig. 5A; data not shown). The maternal chromosome-specific histone H3/H4 acetylation and H3K4 methylation in CGI1 were detected in glial cells and fibroblasts (Fig. 5D). We further analyzed histone H3K27 trimethylation, which is directly regulated by the PcG proteins, because imprinted expression of the major-type *Grb10* transcript was reported to be relaxed in the knockout embryos of the PcG gene, *Eed* (24). In neurons and fibroblasts, H3mK27 was clearly precipitated in CGI1 but not in CGI2 (Fig. 6A). The paternal chromosome-specific methylation of H3K27 was observed in fibroblasts, but a significant allelic difference was not detected in neurons (Fig. 6B). These data suggest that the paternally null expression of the major-type transcript in fibroblasts correlates with paternal chromosome-specific methylation of H3K27 in CGI1. In CGI3, histones H3 and H4 were hypoacetylated and H3K4 was hypomethylated (data not shown). We could not detect significant differences in histone acetylation and methylation in CGI3 between cultured cells.

DISCUSSION

It has been known that mouse *Grb10* shows reciprocal imprinting depending on the tissue-specific promoters. In most tissues, *Grb10* is expressed exclusively from the maternal allele, whereas in the brain, it is expressed predominantly from the paternal allele (1, 17). Such reciprocal imprinting of *Grb10* in a tissue-specific and promoter-specific manner is a good model to elucidate how promoter-specific imprinting is epigenetically controlled in tissues. In this study, we have developed a cell culture system with which cell-type-specific imprinting of *Grb10* can be characterized in the mouse brain. We demonstrated that promoter-specific and developmental stage-specific imprinting of *Grb10* expression in the brain is associated with parental allele-specific epigenetic modifications in brain cell lineages.

Two previous reports described that reciprocal imprinting of *Grb10* occurs in a tissue-specific and promoter-specific manner (1, 17). Our studies with cultured cortical cells revealed that the brain type transcript containing exon 1b was expressed in neurons but not in glial cells, while the major-type transcript containing exon 1a was expressed in all cultured cells, including neurons (Fig. 2C). These findings indicate that the brain-specific promoter actually implies the neuron-specific promoter and that the major-type promoter works as the common promoter in all tissues. Imprinting analysis of these transcripts clearly showed that the brain type transcript is expressed exclusively from the paternal allele and the major-type transcript is expressed exclusively from the maternal allele (Fig. 3). These